

THE DETERMINATION OF THE EVOLUTIONARY PROPERTIES OF QUASARS BY MEANS OF THE LUMINOSITY-VOLUME TEST

*M. Rowan-Robinson**

(Communicated by W. H. McCrea)

(Received 1967 August 3)

Summary

A cosmological test suitable for sources with a large dispersion in luminosity, the luminosity-volume test, is described.

Application to both the optical and radio data for quasars, assuming their redshifts to be cosmological, shows that none of the relativistic models can apply without some evolutionary factor that affects both radio *and* optical properties. Simple evolutionary hypotheses are tested, and it is found that only relatively empty models ($4\pi G\rho_0 \leq H_0^2$) with $-1 \leq q_0 \leq 0.5$ are consistent with power-law luminosity-evolution, whereas all models are consistent with density-evolution. Evolutions with a negative exponential dependence on the scale-factor, which do not require a truncation of the evolving population at finite redshift to give a finite integrated background radiation, represent the data well.

The test should be applicable to radio-galaxies when the data is more complete.

1. *Introduction.* Throughout this work we take the conventional view that the redshifts of quasars are cosmological (1). Although we recognize that severe difficulties exist for this view (2), (4)–(6), the other possible explanations that have been presented in detail to date (8), (9) pose more difficulties than they solve (10)–(12).

Pessimism has been expressed whether, even if quasars are at cosmological distances, they are of much value to cosmology (13), (14). The two classical tests, the magnitude–redshift test and the number-counts of sources, are only effective in distinguishing between cosmological models in situations where the dispersion in luminosity is small. While this is the case for the optical luminosities of galaxies, it is certainly not true for the radio-luminosities of radio-galaxies, or for either the optical or radio luminosities of quasars (we shall drop the qualification ‘if the redshifts of quasars are cosmological’ in the remainder of this paper). We aim to show that this pessimism is unjustified, since the additional factor of completeness down to a limiting flux-level enables a far more powerful test, the ‘luminosity-volume’ test, to be applied. This test combines the essential features of both the redshift–magnitude and number-count tests, and uses more information than either. A simple extension enables evolutionary hypotheses to be tested.

Radio number-counts of *all* sources provide clear evidence that evolutionary factors are affecting at least a sub-population of the sources (15)–(18). Two kinds of evolution have been considered in some detail in earlier interpretations of the radio number-counts (18)–(20):

* Present address: Department of Mathematics, Queen Mary College, London E.1.

(a) *Density evolution.* The fraction of material in the form of active sources is a function of epoch.

(b) *Radio luminosity evolution.* The typical luminosity of sources is a function of epoch, while the fraction of material in the form of active sources and the form of the dispersion of luminosities are independent of epoch.

Longair (18) has shown that to obtain consistency with number-counts to low flux-levels and the extragalactic contribution to the integrated background radio emission *all* classes of source can not be supposed to evolve. If the evolution is then due to an *indistinguishable* sub-population of the sources, the distinction between hypotheses (a) and (b) disappears (18). However if the evolution takes place in a recognizable sub-population (e.g. the quasars) then we are dealing with distinct hypotheses and can hope to test between them. Earlier suggestions that the magnitude–redshift diagram for quasars supported luminosity rather than density evolution (22), (23) were shown to be incorrect (24). The present results are still stronger: luminosity evolution of the form considered in (18)–(20), (22), (23) is inconsistent with a wide range of cosmological models, whereas consistency with all models can be obtained using density evolution.

However, it is important to consider whether results obtained using a particular mathematically simple form of evolution may not depend rather strongly on that mathematical form. The truncation of the evolving population beyond a redshift of about four (18) may fall in this category. In this paper we consider other forms of evolution which do not require such a truncation. It is a matter for subsequent investigation to decide whether such forms of evolution could give consistency with radio number-counts to low flux-levels and with the integrated extragalactic background.

The cosmological models we have tested are the familiar relativistic models. We include the possibility of a non-zero cosmological constant Λ : purists who dislike the cosmological constant may simply examine our results for $\Lambda = 0$.

In Section 12 we also describe the results of testing the steady-state cosmology and a class of Brans–Dicke models.

2. The models

(i) *Summary of properties.* The properties of the relativistic cosmological models are discussed in many standard references, e.g. (25)–(27), but for completeness we summarize here the relations we need.

The observed flux in the frequency range ν_0 to $\nu_0 + d\nu_0$, from a source emitting $F(\nu_e)d\nu_e$ in the corresponding range of emitted frequency ν_e to $\nu_e + d\nu_e$, is given by

$$f(\nu_0)d\nu_0 = \frac{F(\nu_e)d\nu_e(1 + k r_0^2/4)^2}{R_0^2 r_0^2 Z^2} \quad (1)$$

where

$$\frac{\nu_0}{\nu_e} = 1 + z = Z$$

and

$$\int_{t_e}^{t_0} \frac{dt}{R} = \int_0^{r_0} \frac{dr}{1 + k r^2/4} \quad (2)$$

Writing $\mathcal{F} = \log_{10} F(\nu_0)$, $\mathcal{f} = \log_{10} f(\nu_0)$, equation (1) becomes

$$\mathcal{F} = \mathcal{f} + \log_{10} \frac{R_0^2 r_0^2 Z^2}{(1 + k r_0^2/4)^2} - 0.4 K \quad (3)$$

where the K -correction takes account of the selectivity of the atmosphere and the apparatus, and of the shift of the spectrum across the observed frequency band. The forms we have used for optical and radio K -corrections are presented in Appendix I.

From Einstein's equations for uniform, pressure-free universes, the scale-factor $R(t)$ satisfies the equations

$$\dot{R} = -4\pi G\rho R/3 + \Lambda R/3 \quad (4)$$

$$(\dot{R})^2 = 8\pi G\rho R^2/3 + \Lambda R^2/3 - kc^2 \quad (5)$$

where Λ is the cosmological constant and the density, ρ , satisfies the equation

$$\rho R^3 = \rho_0 R_0^3,$$

subscripts zero referring to the present epoch.

Then if we write

$$H = \dot{R}/R, \quad q = -\ddot{R}R/\dot{R}^2, \quad (6)$$

and

$$\sigma = 4\pi G\rho/3H^2, \quad (7)$$

equations (4) and (5) become

$$\Lambda/3 = (\sigma - q)H^2 = (\sigma_0 - q_0)H_0^2 \quad (8)$$

and

$$\begin{aligned} kc^2 &= (3\sigma - q - 1)H^2 R^2 \\ &= (3\sigma_0 - q_0 - 1)H_0^2 R_0^2. \end{aligned} \quad (9)$$

(ii) *Flow diagram for the models.* Writing $Z = R_0/R$, we can use equations (5) (8), (9) to obtain

$$H^2(t) = H_0^2\{\sigma_0 - q_0 + (1 + q_0 - 3\sigma_0)Z^2 + 2\sigma_0 Z^3\} = H_0^2 \cdot Y(Z)$$

$$\sigma(t) = \sigma_0 Z^3 / Y(Z)$$

$$q(t) = \{\sigma_0(Z^3 - 1) + q_0\} / Y(Z).$$

Thus if H_0 , σ_0 , q_0 are known at the present epoch, then H , σ , q are known for all epochs, past and future. The behaviour of the models can be illustrated by a flow diagram (Fig. 1). This diagram, and an illuminating discussion of the σ - q representation, can be found in Refsdal & Stabell (28). For our purposes the interesting feature to note is that there are just three fixed points in this diagram: the Einstein-de Sitter model ($\sigma = q = 1/2$), the de Sitter model ($\sigma = 0$, $q = -1$), and the Milne model ($\sigma = q = 0$). These represent asymptotic states of the Universe: the Einstein-de Sitter model is the initial state of all non-empty models except those to the left of the curve A, while the Milne and de Sitter models are the final states of monotonic expanding models (all those to the left of the curve B) with $\Lambda = 0$ and $\Lambda \neq 0$, respectively. Oscillating models are those to the right of the curve B. A and B correspond to those models which approach the Einstein static universe as $t \rightarrow \pm \infty$ respectively (i.e. A is the Eddington-Lemaitre model).

The loci to the left of the curve A correspond to those models which 'bounce' under the action of cosmological repulsion. As Solheim (29) has remarked, most of these models are ruled out if the redshifts of quasars are cosmological, since they give upper limits to Z which are inconsistent with values already obtained for

quasars. In fact for these models to be correct we must be indistinguishably close to the de Sitter model at the present epoch. Their philosophical attraction is that they are the only non-empty models which do not possess a singularity.

From the point of view of the testing of models, the most interesting situations arise if (σ_0, q_0) are *not* near any of the three fixed points. For then we know the future of the Universe and its past history (at least back to the epoch where the pressure becomes significant). But if (σ_0, q_0) are near to one of the fixed points in the σ - q plane, we cannot tell whether the Universe has always had these values of σ and q , or whether it is in an asymptotic state.

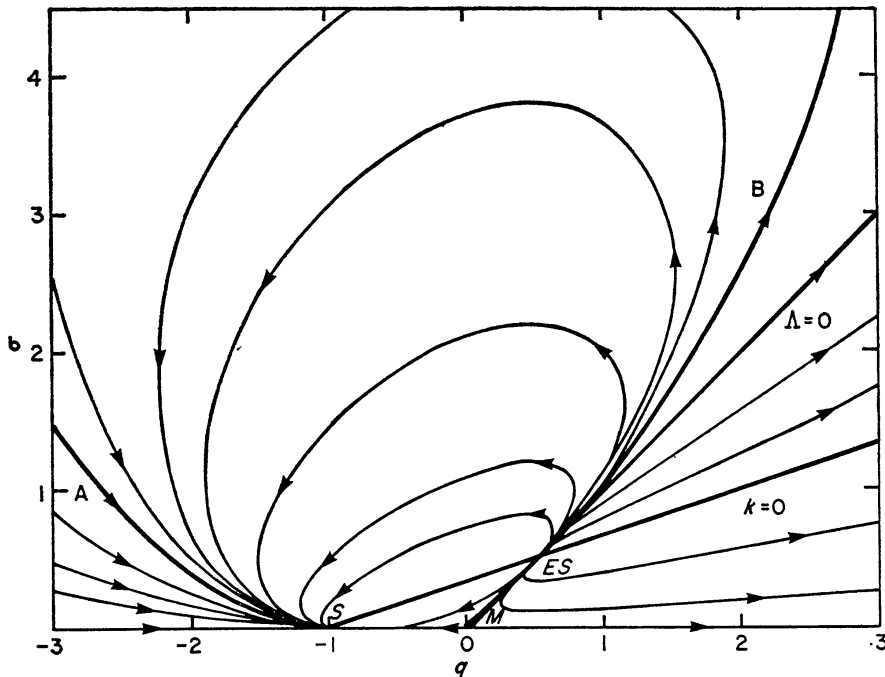


FIG. 1. Flow diagram for the models. Loci to the right of *B* are oscillating models; those to the left of *A* have 'bounced' under the action of cosmological repulsion; those between *A* and *B* are monotonic expanding models. The three fixed points are the Einstein-de Sitter (*ES*), Milne (*M*), and de Sitter (*S*) models. The directions indicated by the arrows correspond to expansion of the Universe.

The smoothed-out density of the material actually observed to date ($7 \times 10^{-31} \text{ g cm}^{-3}$) (30), and the present value of the Hubble constant ($H_0^{-1} = 1.2 \times 10^{10}$ years), suggest that our present position in the σ - q plane may be rather close to the $\sigma = 0$ axis. Difficulties in reconciling the ages of the oldest stars with the age of the Universe may force us to the left of the point *M* and perhaps rather near to the point *S*. But considerations of this kind are subject to enormous uncertainty.

3. Influence of volume effect on magnitude-redshift test

(i) *Magnitude-redshift test.* The results of attempts to distinguish between these models using the magnitude-redshift test for the brightest galaxies in clusters have been reviewed and extended by Solheim (29), who has computed exact theoretical relations instead of the power-series expansions used in earlier work (31), (32). His best values for the cosmological parameters are

$$q_0 = -0.06, \quad \sigma_0 = 4.53,$$

though these values are appreciably modified if the galaxies are assumed to change their luminosity with epoch (29), (33).

The acceptable models appear as a region of the $\sigma_0 - q_0$ plane (the 'model' diagram). He also applies this procedure to optical data for fifteen quasars. However it is necessary to take account of the severe selection effect imposed by the limiting radio magnitude for these objects (nine flux-units if we confine our attention to identifications from the 3C catalogue (37), (38)), and also of the 'volume effect' discussed below. In the present work we have rather more data available (37 redshifts), we take account of these selection effects, and we also perform the test in a different and more powerful way.

A number of other authors have discussed the observational data for quasars with respect to particular cosmological models. McCrea (34) plotted the absolute optical magnitudes of quasars against redshift for three models: the Milne model ($\sigma_0 = q_0 = 0$), the de Sitter model ($\sigma_0 = 0, q_0 = -1$; the steady-state model gives the same diagram), and a particular model used by Schmidt for which $\sigma_0 = q_0 = 1$. McCrea pointed out that the luminosity, $F_1(z)$ say, of the most luminous source out to redshift z should be an increasing function of z , simply as a probability effect. The Schmidt model then seemed to be rendered improbable by the fact that the nearest quasars, 3C273, would be intrinsically the most luminous, in this model. The rate of increase of $F_1(z)$ appeared improbably steep in the steady-state model, on the other hand.

(ii) *The volume effect.* Some quantitative estimate of the importance of the effect may be made as follows. We assume that the proper number-density of quasars at any epoch, $\zeta(t)$, is proportional to the smoothed-out cosmological density, $\rho(t)$, and that the luminosity-function (18) for quasars is independent of epoch. That is, at epoch t let the number of sources per unit proper volume having log $_{10} F$ in the range

$$\mathcal{F} \text{ to } \mathcal{F} + d\mathcal{F} \text{ be } \zeta(t) \cdot \phi(\mathcal{F}) d\mathcal{F}$$

where

$$\int_{-\infty}^{+\infty} \phi(\mathcal{F}) d\mathcal{F} = 1.$$

Define the coordinate number-density,

$$\eta(t) = \zeta(t) \cdot \frac{R^3(t)}{R_0^3}:$$

thus if $\zeta(t) \propto \rho(t)$, then $\eta(t) = \text{const} = \eta(t_0) = \eta_0$, say. The element of proper volume is

$$\frac{R^3(t) r^2 dr \sin \theta d\theta d\phi}{(1 + k r^2/4)^3}$$

so the total number of sources in the range of luminosity \mathcal{F} to $\mathcal{F} + d\mathcal{F}$ out to redshift z is

$$N(\mathcal{F}, z) d\mathcal{F} = \eta_0 R_0^3 \cdot V(z) \cdot \phi(\mathcal{F}) d\mathcal{F}$$

where

$$V(z) = \int_0^{r_0(z)} \frac{4\pi r^3 dr}{(1 + k r^2/4)^3}$$

Then the expected luminosity, $F_N(z)$, of the N th most luminous source out to

redshift z will be roughly the solution of the equation

$$\eta_0 R_0^3 \cdot V(z) \cdot y \int_{\mathcal{F}_{N(z)}}^{\infty} \phi(\mathcal{F}) d\mathcal{F} = N,$$

where $\mathcal{F}_{N(z)} = \log_{10} F_N(z)$, and y is the fraction of the sky covered by the sources.

Let

$$\Phi(x) = \int_{-\infty}^{\infty} \phi(\mathcal{F}) d\mathcal{F}$$

Then

$$\mathcal{F}_{N(z)} = \Phi^{-1} \left\{ 1 - \frac{N}{\eta_0 R_0^3 \cdot V(z) \cdot y} \right\},$$

where

$$\Phi^{-1}\{\Phi(x)\} = x. \quad (10)$$

For example if (a)

$$\phi(\mathcal{F}) = \frac{1}{\sqrt{2\pi}a} \cdot \exp \left\{ -(\mathcal{F} - \mathcal{F}_0)^2 / 2a^2 \right\}$$

Then

$$\mathcal{F}_{N(z)} = \mathcal{F}_0 + a \operatorname{erf}^{-1} \left\{ 1 - \frac{N}{\eta_0 R_0^3 V(z) y} \right\}$$

and if (b)

$$\phi(\mathcal{F}) = b (\log_e 10) 10^{-b(\mathcal{F} - \mathcal{F}_1)} \quad \text{for } \mathcal{F} \geq \mathcal{F}_1 \\ \text{for } \mathcal{F} < \mathcal{F}_1$$

then

$$\Phi(\mathcal{F}) = 1 - 10^{-b(\mathcal{F} - \mathcal{F}_1)},$$

and

$$\mathcal{F}_{N(z)} = \mathcal{F}_1 + \frac{1}{b} \log_{10} \left\{ \frac{R_0^3 y \eta_0 V(z)}{N} \right\} \\ = \text{const.} + \frac{1}{b} \log_{10} V(z).$$

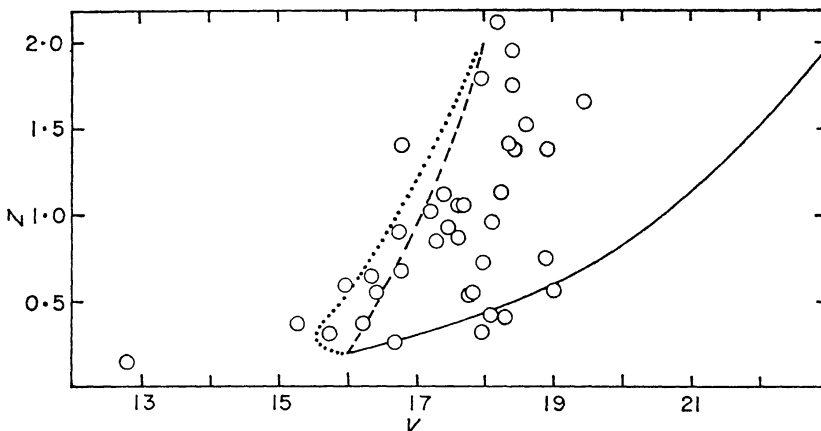


FIG. 2. Magnitude (V)-redshift (z) diagram for quasars showing 'volume effect'. The continuous line is the theoretical magnitude-redshift curve for the de Sitter model. The other two curves show the shapes of the predicted loci of brightest sources in this model for simple luminosity functions: dotted curve, Gaussian with dispersion of two magnitudes; broken curve, exponential dependence on luminosity, $F(\nu\nu)$, with index -1.5 (to base 10). These forms are chosen only to give a similar shape to the upper envelope for the observational points (circles), and are not necessarily consistent with the data.

Some idea of the importance of the volume effect for the optical redshift–magnitude diagram for quasars may be gained from Fig. 2, which shows $F_1(z)$ for two simple luminosity functions of type (a) and (b), in the de Sitter model. The parameters chosen are $a = 0.8$, $b = 1.5$, $4\pi\eta_0\gamma = 10^{-3}$ per $(c/H_0)^3$.

We are not claiming that the optical luminosity function for quasars is actually of either of these forms, but merely demonstrating how severe the effect of a large dispersion in luminosity can be. Clearly a large part of the divergence of the data from the normal de Sitter m – z curve could be ascribed to this effect, so that analysis of the kind performed by Solheim (29) is unlikely to give accurate results for quasars. However if from counts and from identifications we can obtain information about η_0 and the form of $\phi(\mathcal{F})$, then it is in principle possible to test cosmological models by comparing equation (10) with the observed locus of the N th most luminous source out to redshift z , for different values of N . In practice this is unsatisfactory, since η_0 and $\phi(\mathcal{F})$ cannot be at all accurately determined. The test we shall describe in section takes full account of the volume effect, but does not require knowledge of η_0 or $\phi(\mathcal{F})$.

McVittie & Stabell (35) have also considered plots of the optical luminosity of quasars against redshift in several models and argue that although evolution would be necessary in models with $q_0 = \sigma_0 = 0$ and $q_0 = \sigma_0 = 1$, this is not the case for the model $q_0 = 1$, $\sigma_0 = 3$, for example. In Section 5 we show that *none* of the relativistic models are consistent with the present data for quasars, without some kind of evolutionary factors.

McVittie & Stabell (35), and Kafka (14) have allowed for the volume effect in a rather different manner from that described above. Confining their attention to a fixed range of optical luminosity they compare the number of sources out to redshift z with $V(z)$. This is equivalent to the ‘luminosity-volume’ test we describe in the next section, but is limited in two ways. Firstly it does not take account of the serious selection effect imposed by the 3C limiting flux-level.* And secondly it uses the available information in such an inefficient way that, as Kafka admits, no conclusions of real statistical significance can be drawn with the present data.

Rees & Sciama (36) showed that in different ranges of radio luminosity in the steady-state model there was an excess of quasars at large redshift. The inconsistency is even more striking when correction is made for the effect of optical selection, and when the optical luminosities are also considered.

4. *Luminosity-volume test.* The central suggestion of this paper is that for quasars the magnitude–redshift test be replaced by the ‘luminosity-volume’ test. Suppose that (i) the number of quasars per unit proper volume, $\zeta(t)$, is proportional to the smoothed-out cosmical density at that epoch; (ii) the distribution of luminosities of quasars (i.e. the form of $\phi(\mathcal{F})$) is the same at all epochs.

Then the total number of sources out to the epoch corresponding to redshift z is

$$N(z) = \int_{-\infty}^{+\infty} N(\mathcal{F}, z) d\mathcal{F} = \eta_0 R_0^3 \cdot V(z) \quad (11)$$

$V(z)$ is the comoving coordinate volume of the sphere bounded by sources whose light is redshifted by z .

* In more recent work Kafka (54) now takes account of the selection effect but still does not combine the information in an efficient enough way to obtain significant results.

Then in any particular model that we wish to test we consider the distribution of luminosity \mathcal{L} (see equation (3)) with respect to volume V : that is, we transform the magnitude-redshift diagram to a luminosity-volume diagram. If assumptions (i) and (ii) hold, we should expect to find, in any given range of luminosity, equal numbers of sources in any two equal volumes of comoving coordinate space. However as a result of the limitations of our telescopes, not all quasars are visible. Confining our attention to 3C quasars, only those brighter than the limiting flux-level are visible. An optical identification can then only be made if the quasar is brighter than the limiting optical magnitude. Moreover the degree of complete-

TABLE I

3C	z	f_{rad}	V	K_v	$V+K_v$	α
273	0.158	-24.14	12.80	-0.64	12.16	0.35
323.1	0.260	-25.02	16.69	-0.45	16.24	0.64
249.1	0.311	-24.91	15.72	-0.36	15.36	0.87
277.1	0.320	-24.89	17.93	-0.35	17.58	0.92
48	0.367	-24.30	16.20	-0.28	15.92	0.50
351	0.371	-24.93	15.28	-0.27	15.01	0.60
215	0.411	-24.97	18.27	-0.22	18.05	1.00
47	0.425	-24.67	18.10	-0.21	17.89	0.89 (K)
279	0.536	-24.70 (3C)	17.75	-0.13	17.62	0.54 (K)
147	0.545	-24.21	17.80	-0.12	17.68	0.45
334	0.555	-24.97	16.41	-0.12	16.29	0.78 (K)
275.1	0.557	-24.77	19.00	-0.12	18.88	0.88
345	0.594	-24.97	15.96	-0.10	15.86	0.24 (K)
263	0.652	-24.86	16.32	-0.06	16.26	0.88
380	0.691	-24.21	16.81	-0.04	16.77	0.77 (K)
254	0.734	-24.69	17.98	-0.02	17.96	0.93 (K)
138	0.754	-24.70	18.84	0.00	18.84	0.38 (K)
286	0.846	-24.65	17.30	+0.02	17.32	0.15
196	0.872	-24.20	17.60	+0.02	17.62	0.70
309.1	0.903	-24.74	16.78	+0.02	16.80	0.45 (K)
336	0.927	-24.84	17.47	+0.02	17.49	0.87
288.1	0.960	-24.99	18.12	+0.01	18.13	0.93
245	1.029	-24.99	17.25	0.00	17.25	0.61 (K)
287	1.054	-24.82	17.67	-0.01	17.66	0.48 (K)
186	1.063	-24.84	17.60	-0.01	17.59	1.18
204	1.112	-24.99	18.21	-0.02	18.19	1.05
208	1.112	-24.77	17.42	-0.02	17.40	0.98 (K)
181	1.382	-24.86	18.92	-0.10	18.82	0.94
268.4	1.400	-25.02	18.42	-0.10	18.32	0.69
446	1.403	-24.74 (3C)	18.39	-0.10	18.29	0.53 (K)
298	1.436	-24.33	16.79	-0.11	16.68	0.98 (K)
270.1	1.519	-24.89	18.61	-0.13	18.48	0.69
280.1	1.659	-24.83	19.44	-0.15	19.29	1.09
454	1.756	-25.02	18.40	-0.14	18.26	0.73
432	1.804	-24.91	17.96	-0.14	17.82	1.04
191	1.946	-24.95	18.40	-0.12	18.28	0.98 (K)
9	2.012	-24.77	18.21	-0.09	18.12	1.02

- Notes: (i) Redshifts and optical magnitudes from Refs (7), (41) and (42).
(ii) Radio fluxes from 3CR (38), except those marked (3C), which are from 3C (37).
(iii) K_v taken from Sandage (52).
(iv) Sources classified by Kellerman (50) as having straight spectra marked (K).
The rest calculated as in Appendix I.

ness of the identifications may be different in different ranges of magnitude, an effect which could be reinforced by non-random selection of objects for redshift measurements. However, although such effects may well be present, it is not necessary that the set of quasars with known redshift at our disposal be complete, but only that it be representative down to the limiting flux-levels. Throughout this work we assume that the set of 37 quasars listed in Table I are representative down to the 3C limiting flux-level of nine flux-units, and down to the 18th visual magnitude.

Penston & Rowan-Robinson (3) have suggested that the 3C quasars with visual magnitudes fainter than 18 are not distributed isotropically on the sky. Preferring to suppose that this is some effect of observational selection that the Universe is inhomogeneous on the large scale (39), we shall make a correction for this effect at a later stage. For the moment we treat our set of quasars as if it were representative down to the 19th magnitude, which, since there are only two quasars with $V > 19$ in our set, we shall regard as the limiting magnitude for quasars.

Fig. 3 shows optical and radio luminosity-volume diagrams for a particular cosmological model (the Einstein-de Sitter model). The cutoffs imposed by the limiting flux-levels are calculated by eliminating z between

$$\hat{\mathcal{F}} = \hat{f} + \log_{10} \frac{R_0^2 r_0^2 (1+z)^2}{(1+kr^2/4)^2} - 0.4 K(z) \quad (12)$$

and

$$\hat{v} = v(z) \quad (13)$$

where \hat{f} is the limiting flux-level and K the appropriate K -correction (see Appendix I: the radio cut-off is shown for sources with spectral index $\alpha = 0.8$).

Clearly, a source with luminosity \mathcal{F} and redshift z will only be observable if $v(z) \leq \hat{v}(\mathcal{F})$. A difficulty here is that in the radio case, $\hat{v}(\mathcal{F})$ is different for sources with different spectral indices. But the error introduced by taking the radio cutoff to be that appropriate to sources with the mean spectral index (about 0.8) is not very great: a few sources with steep spectra might be missed.

The vertical lines to the right of the two diagrams correspond to a redshift of 2.2, beyond which no quasar has yet been observed. Thus in the radio diagram the line $A_1A_2A_3$ bounds the observable region of the luminosity-volume plane. If we define the line $B_1B_2B_3$ by the relations

$$v = v(2.2)/2 \text{ for } \mathcal{F} \geq \hat{\mathcal{F}}(2.2)$$

and

$$v = \hat{v}(\mathcal{F})/2 \text{ for } \mathcal{F} < \hat{\mathcal{F}}(2.2),$$

then $B_1B_2B_3$ divides $A_1A_2A_3$ into two regions in which, under assumptions (i) and (ii), we should expect to find equal numbers of sources.

Before we compare the numbers of quasars actually found in such equivalent regions, we have to allow for the fact that the set of quasars in $A_1A_2A_3$ is affected by optical selection. Sources which are intrinsically faint optically can only be found at small redshifts on account of the *optical* cutoff. Similarly the optical diagram is affected by radio selection, since sources intrinsically faint radio-wise can only be found at small redshifts on account of the *radio* cutoff.

For a set of sources free from optical selection out to redshift z_1 we should

confine our attention to sources with $\mathcal{F}_{\text{opt}} \geq \hat{\mathcal{F}}_{\text{opt}}(z_1)$. For $z_1 = 2.2$ this would be very restrictive, but we can relax this requirement considerably without much loss of accuracy. In Fig. 3(b) we show $\mathcal{F}_{\text{opt}} = \hat{\mathcal{F}}_{\text{opt}}(1.4)$, for example (the broken line). Optical selection operates against sources falling in the shaded region in

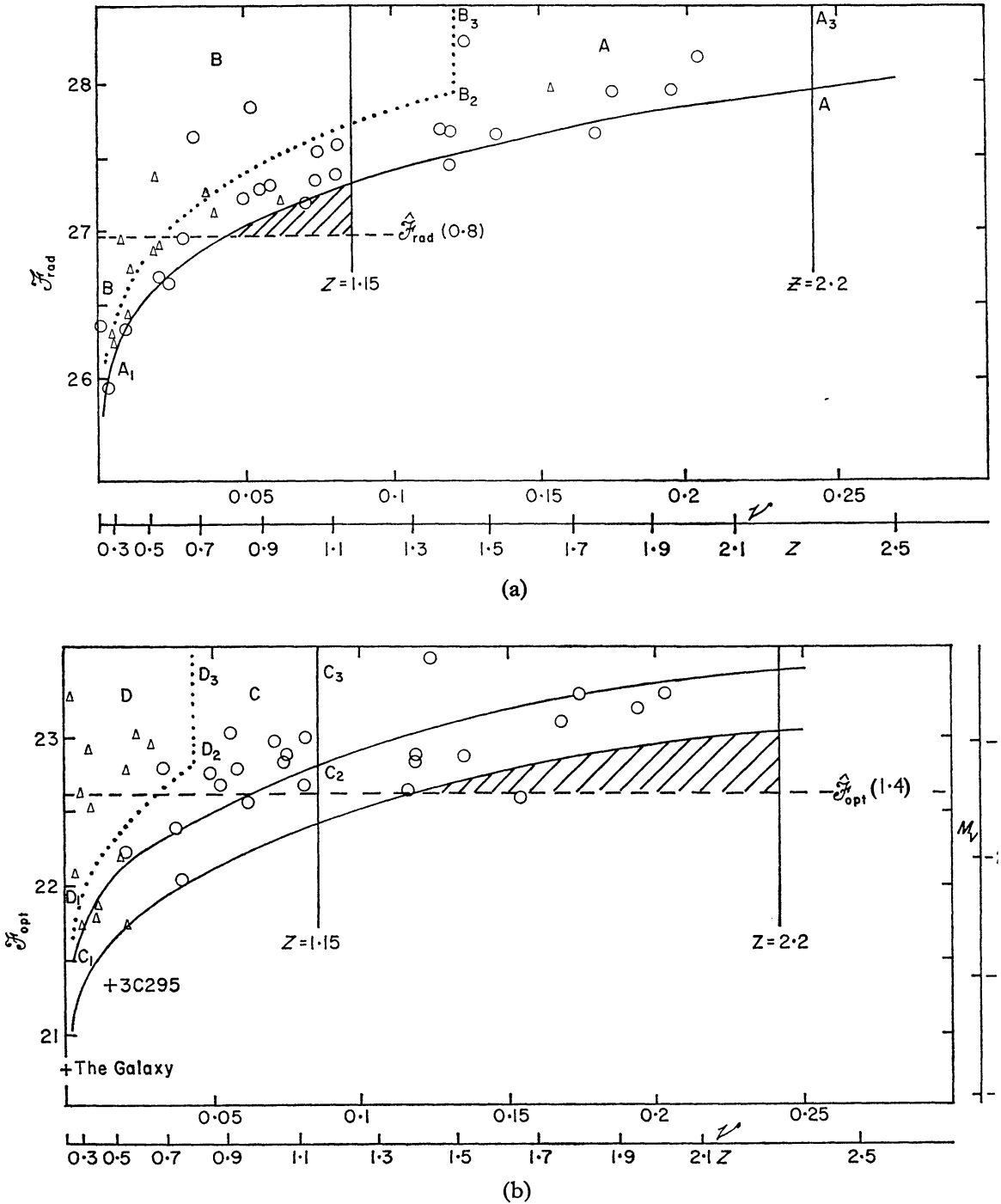


FIG. 3. Radio (a) and optical (b) 'luminosity-volume' diagrams for quasars in the Einstein-de Sitter model. A_1A_2 corresponds to the 3C cutoff of nine flux-units, C_1C_2 to a visual magnitude of 18. In (a) circles/triangles are those quasars with $\mathcal{F}_{\text{opt}} \geq \hat{\mathcal{F}}_{\text{opt}}(0.8)$ respectively: in (b) circles/triangles are those quasars with $\mathcal{F}_{\text{rad}} \geq \hat{\mathcal{F}}_{\text{rad}}(1.4)$. Units of \mathcal{F} are log₁₀ watts/(c/s).

Fig. 3(b), since they would have $V > 19$. It seems unlikely that very many sources are 'missing': moreover these would all fall in the farther of the two regions of space described above. Since it transpires that there are significantly more quasars in this further region for all the relativistic cosmologies, our conclusions are merely reinforced.

Similarly, for a set of quasars free from radio selection out to z_2 we should confine our attention to sources with $\mathcal{F}_{\text{rad}} \geq \mathcal{F}_{\text{rad}}(z_2)$. In view of the probable incompleteness of the identifications for $18 < V \leq 19$, we shall apply the optical luminosity-volume test to sources with $V \leq 18$ only.* Since only two out of our 37 sources have $V \leq 18$ and $z > 1.15$, presumably due to radio selection, we take $z_2 = 1.15$. The line $C_1C_2C_3$ now bounds the region of interest in Fig. 3(b). A set of quasars mainly free from radio selection out to redshift 1.15 can be obtained by demanding $\mathcal{F}_{\text{rad}} \geq \mathcal{F}_{\text{rad}}(0.8)$: a few sources in the shaded region of Fig. 3(a) would be missed. The point of this procedure is that for the price of a small remaining effect of selection we more than double the number of quasars available for testing. The conclusions have been found to be insensitive to the actual parameters chosen.

Finally, the line $D_1D_2D_3$ in Fig. 3(b) is defined by

$$v = \hat{v}(\mathcal{F})/2 \quad \text{for } \mathcal{F} < \mathcal{F}_{\text{opt}}(1.15)$$

and

$$v = v(1.15)/2 \quad \text{for } \mathcal{F} \geq \mathcal{F}_{\text{opt}}(1.15).$$

Then if n_A, n_B, n_C, n_D are the numbers of quasars found in the regions A, B of Fig. 3(a) and C, D of Fig. 3(b), respectively, we expect $n_A = n_B, n_C = n_D$, if hypotheses (i) and (ii) are satisfied. To test whether the numbers obtained are consistent with these expectations, we compare the quantity

$$\frac{(n_A - n_B)^2}{(n_A + n_B)} + \frac{(n_C - n_D)^2}{(n_C + n_D)}$$

with the χ^2 variable with two degrees of freedom. A probability can then be assigned, from this combined radio and optical luminosity-volume test, to the chosen cosmological model under assumptions (i) and (ii).

5. *Relativistic cosmological models without evolutionary effects.* The procedure described above has been applied, with the aid of a computer, to a grid of cosmological models in the range: $-1 \leq q_0 \leq 3, 0 \leq \sigma_0 \leq 3$, which includes most of the region of interest in the $\sigma_0 - q_0$ plane.

Recently Lemaitre's models have been re-advocated (40): these lie to the right of but close to curve A in Fig. 1, and have the possibility of an antipole. Whereas $\hat{\mathcal{F}}(z)$ is monotonic increasing for most models, in certain models it can reach a maximum and then start to decrease, eventually tending to zero at the antipole.

* It may seem logically unsatisfactory to take the optical limiting magnitude as 19 when correcting the radio-data for optical selection, and as 18 when performing the optical luminosity-volume test. However in the latter case it is necessary only that we choose some magnitude brighter than or equal to the actual limiting magnitude, so our procedure is certainly consistent if the data is representative in the range $18 < V \leq 19$ (though wasteful of information). On the other hand if our set of quasars is incomplete in the range $18 < V \leq 19$, then the effect is much severer for the optical luminosity-volume test than for the correction of the radio-data for optical selection, since many of the 'missing' sources would be excluded anyway from the radio test by the condition $\mathcal{F}_{\text{opt}} \geq \mathcal{F}_{\text{opt}}(1.4)$.

Although these exotic models have to be considered individually and are not immediately amenable to the procedure described in the previous section, it may well be that the range of parameters we have considered includes all the serious possibilities. Actually we have tested models with larger values of σ_0 and q_0 , but these give no new results and anyway imply unreasonable values for the average density of the Universe and the total age of the Universe.

The formulae used are summarized in Appendix II: a detailed discussion can be found in Solheim's paper (29). Our results are presented in Fig. 4(a), which

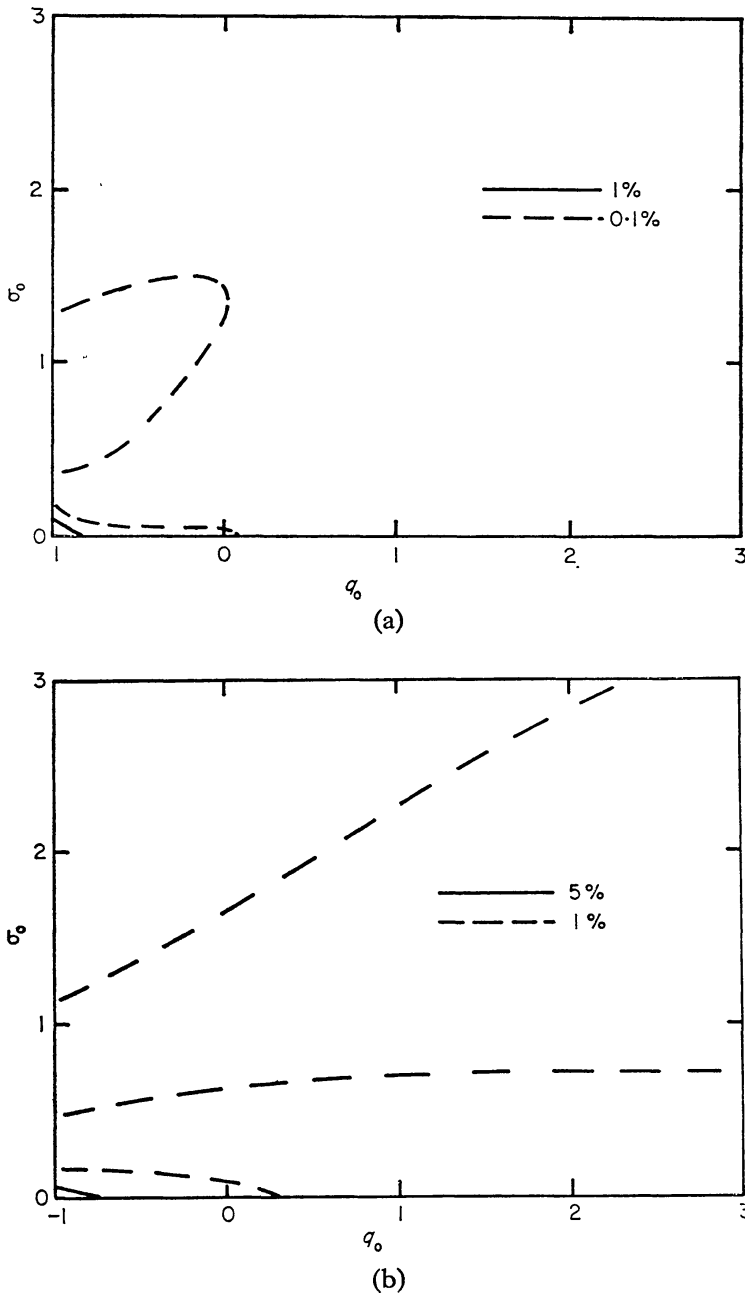
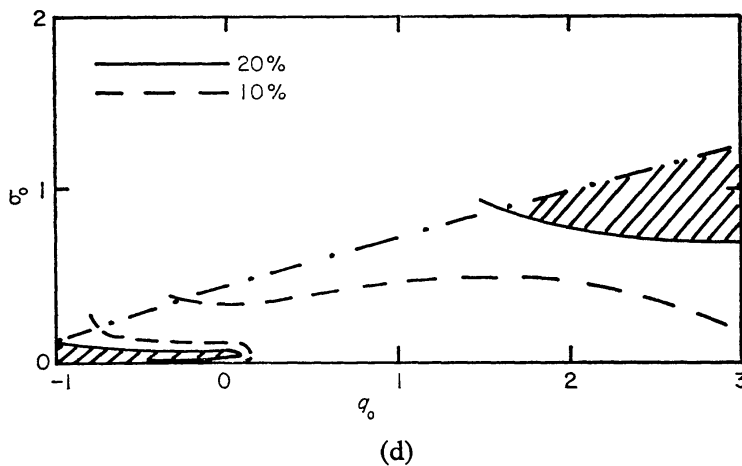
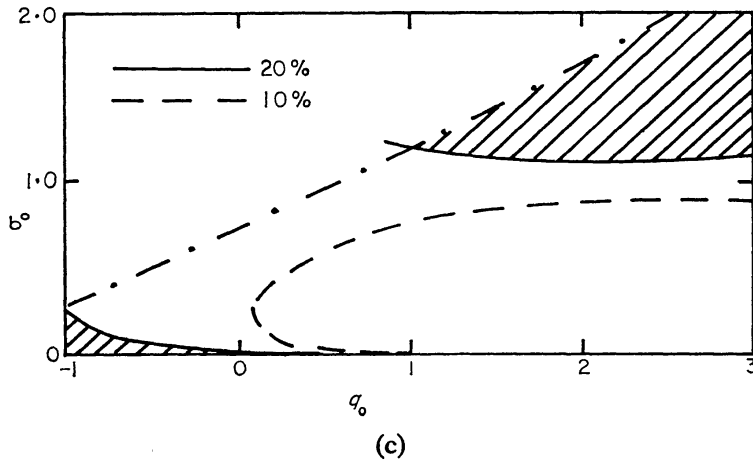


FIG. 4. Model diagram: $\sigma_0 - q_0$: (a) no evolution, optical and radio luminosity-volume tests combined; (b) no evolution, optical test only; (c) power-law luminosity evolution, $Q_L = 2.5$, combined optical and radio tests; (d) as in (c) but with $Q_L = 3.0$. Dash-dotted lines in (c), (d) and Figs 7-10 correspond to the maximum rate of luminosity evolution discussed in Section 8. The contours join models with equal probability of being correct.



shows interpolated contours of equal probability in the $\sigma_0 - q_0$ plane. No model gives a probability above a few per cent, so we may conclude with some confidence that none of these models are consistent with the present data for quasars. Here we are at odds with McVittie & Stabell (35), who consider that the model with $q_0 = 0$, $\sigma_0 = 3$ is acceptable. Our procedure assigns a probability of less than 0.01 per cent to this model. Evolutionary factors must be affecting the distribution of quasars if *any* of the relativistic models are to apply.

In Fig. 4(b) we plot the contours of equal probability if the optical luminosity-volume alone is applied (suitably corrected for the effects of radio-selection). Although the probabilities are rather higher from this weaker test, all the models are ruled out at the 10 per cent level of significance. The least inconsistent models are those near to the de Sitter model ($\sigma_0 = 0$, $q_0 = -1$). These results should be compared with those of Solheim from applying the magnitude-redshift test to the cluster data of Baum (32) and Humason, Mayall & Sandage (31). His outermost contour includes an area of the $\sigma_0 - q_0$ plane very much larger than the whole of that which we have considered, yet corresponds to a probability of nearly 40 per cent. Such a comparison demonstrates the great power of the luminosity-volume test, given a set of objects like the quasars to which it can be applied.

The fact that the optical data alone is inconsistent with all the models considered demonstrates that the evolutionary factors required cannot be such as to affect the radio-emission alone. Thus the simplest form of the luminosity-evolution

hypothesis is insufficient, namely that the fraction of cosmical material in the form of quasars is the same at each epoch but the typical radio luminosity was greater in the past. Our analysis demonstrates that if the number-density of quasars at any epoch is proportional to the smoothed out cosmological density at that epoch, then *the typical optical luminosity must also have been greater in the past*, for the relativistic models to apply. Presumably the optical and radio emissions would then have to arise from a common mechanism. The evidence for a relationship between optical and radio luminosity is discussed in Section 7.

An alternative, and perhaps simpler, explanation is that the fraction of material in the form of quasars is a decreasing function of the cosmical time. In either case, we may predict that if optical counts can be performed on a complete set of quasars, free from radio selection (e.g. if optical or infrared (49) searches of the sky are performed), then those counts will give a $\log N$ - $\log S$ slope steeper than -1.5 . Since optical counts by Sandage (41) down to 18.5 magnitudes of the Haro-Luyten catalogues of blue objects give a slope rather less steep than -1.0 ($d \log N/dm_{pg} = 0.38$), we may deduce that these quasars do not make a *dominant* contribution to those catalogues at 18.5 m. But a *substantial* contribution is, of course, not ruled out by this argument. Or putting the argument another way, if the quasars *do* make a dominant contribution to the Haro-Luyten catalogues at faint magnitudes, then we have to rule out either the cosmological interpretation of the redshifts of quasars, or the relativistic cosmologies.

Before attempting to set some limits on the evolutionary parameters required to obtain consistency with relativistic models, we discuss some of the physical factors which might give rise to evolutionary effects. Some unrealistic assumptions made for reasons of mathematical simplicity may well vitiate some of the conclusions of earlier investigations.

6. *Possible evolutionary factors affecting the distribution of quasars.* Since only a small fraction of the available material at any epoch appears to be in the form of active quasars, it is quite uncertain that this fraction should be the same at different epochs. However we may distinguish two situations of particular interest:

6.1 *Quasars are violent outbursts in pre-existing agglomerations of matter.* Such a view links them with the strong radio-galaxies, which they resemble in total radio power, in radio spectra, and in certain cases, in radio structure (e.g. 3C47). It is then reasonable to suppose that the fraction of matter in the form of active quasars at any (recent) epoch is independent of epoch. But this is certainly not necessary, for evolution in number-density $\eta(t)$ may arise if the probability that an object has an outburst between epochs t and $t+dt$, $p(t) dt$, is a function of epoch, or if the typical lifetime of a source is a function of epoch.

Luminosity evolution may also occur, that is, the typical luminosity of a source may be a function of epoch.

The objects undergoing the outbursts must then have some knowledge of the cosmical epoch. Either they were all born simultaneously and are aware of their age (through some internal evolution), or the outbursts (and/or the associated radiation) are the results of interaction with uncondensed material whose properties change with epoch. Theories of the latter kind might be suitable for radio-galaxies if it transpires that they too must evolve, since their radio-emission is often centred far from the optical galaxy. But they do not seem very likely for the very compact

quasars, particularly as we have shown that the typical optical luminosity is required to be greater in the past if there is no evolution in number-density.

We shall investigate two simple mathematical forms of luminosity evolution:

- (a) $\bar{F}(t) \propto R(t)^{-Q_L}$, which we can write $\bar{F}(z) \propto (1+z)^{Q_L}$
 (b) $\bar{F}(t) \propto \exp(-\text{const. } R(t))$, which we can write

$$\bar{F}(z) \propto \exp \left\{ (1+z_L) \cdot \left(1 - \frac{1}{1+z} \right) \right\}.$$

For the cosmological models considered by Davidson & Davies (20), (21) in which $R(t)$ has a power law dependence on the cosmical time t , our form of evolution (a) is equivalent to that considered by Davidson & Davies, namely a power law dependence of luminosity on cosmical time. Of the relativistic cosmological models, only the Einstein-de Sitter model, with $R(t) \propto t^{2/3}$, is of the form considered by Davidson & Davies, so that only their results for this model can be compared with this work.

The disadvantage of evolutions of the form (a) is that they must be truncated at some finite value of z , z^* say, in order that a finite background radiation be obtained. Davidson & Davies (20) choose for z^* the point at which

$$\frac{d}{dz} \{ \hat{\mathcal{F}}(z) - Q_L \log_{10} (1+z) \} = 0,$$

which seems a completely arbitrary assumption and may strongly influence their conclusions. Longair (18) takes z^* as a parameter to be fitted to the observations, and requires a value for z^* of about three to obtain consistency with the source-counts and the integrated background in the Einstein-de Sitter model.

But unless there are strong physical grounds for considering evolutions of the form (a), it seems rather premature to conclude that there is a real dearth of sources beyond $z = 3-4$ (18). An example of a form of evolution that does not require such a truncation is provided by form (b), where the typical luminosity at any epoch declines exponentially with epoch. We investigate this form in order to demonstrate that definitive conclusions can not be obtained by confining attention to form (a) only, rather than for any special merit in an exponential evolution. The actual form of evolution can not really be determined until the structure of the sources has been settled. But as an illustration of the way different models for the emission might give rise to different evolutionary parameters, we note that:

$Q_L = 3$ corresponds to $\bar{F}(t) \propto \rho(t)$, which could arise if the emission were the result of the interaction of high-velocity shocks or ejected material with intergalactic material;

$Q_L = 3.5$ corresponds to $\bar{F}(t) \propto H(t)^{(1+y)/2}$, $H(t) \propto R(t)^{-2}$, $y = 2.5$, which could arise if the emission were the synchrotron radiation of electrons with a power-law energy spectrum of index 2.5, in a universal magnetic field: as the Universe expands the magnetic pressure is supposed to expand adiabatically ($H^2 R^4 = \text{constant}$).

6.2 *Quasars correspond to the formation of galaxies.* If galaxies burn up some 20 per cent of their hydrogen during the final stages of their formation, perhaps inside massive objects, then objects emitting energy at about the rate found in quasars would be expected (43). If this stage is short compared with cosmological

time-scales, then the number-density of quasars would be proportional to the rate of galaxy formation. In this case it would be extremely unreasonable to suppose that the number-density of quasars is independent of epoch. For comparison, the rate of star-formation is often taken to have a power-law dependence on the gas density. Or perhaps an exponential dependence would be more appropriate. We have tested both of the forms:

$$(c) \quad \eta(t) \propto (1+z)^{Q_D}$$

$$(d) \quad \eta(t) \propto \exp \left\{ (1+z_D) \left(1 - \frac{1}{1+z} \right) \right\}, \text{ where } Q_D, z_D \text{ are parameters.}$$

Evolution (c) has to be truncated at some z^* , but not form (d).

7. *Modified luminosity-volume test.* In order to test cosmological models when evolutionary effects of the kind discussed in the preceding section are present, we modify the luminosity-volume diagrams in a simple way, described in Ref. (24). We consider the distribution of 'corrected' luminosity, \mathcal{F}' , with respect to 'weighted' volume, V' . Assuming that the increase of luminosity with redshift is the same for all classes of quasars, we divide out this increase and compare the distribution of the luminosities as they would be at the present epoch in different ranges of volume weighted by the postulated increase in number-density with redshift. Thus for the four types of evolution suggested in the previous section:

$$(a) \quad \mathcal{F}' = \mathcal{F} - Q_L \cdot \log_{10} (1+z)$$

$$(b) \quad \mathcal{F}' = \mathcal{F} - (1+z_L) \left(1 - \frac{1}{1+z} \right) \log_{10} e$$

$$(c) \quad V' = \int_0^{r_0} \frac{4\pi r^2 (1+z)^{Q_L} dr}{(1+k r^2/4)^3}$$

$$(d) \quad V' = \int_0^{r_0} \frac{4\pi r^2 \cdot \exp \left\{ (1+z_D) \cdot \left(1 - \frac{1}{1+z} \right) \right\} dr}{(1+k r^2/4)^3}.$$

Now it is an assumption underlying our analysis that the radio and optical luminosities are independent. Since we are requiring radio and optical luminosities to be influenced by the same evolutionary factors in cases (a) and (b), we need to consider whether there is a detailed correlation between radio and optical luminosities. Such a correlation might appear if the optical and radio emissions were produced by the same mechanism, and would invalidate results obtained by the modified luminosity-volume test. In Fig. 5 we have plotted the optical against radio luminosity for quasars with $z \leq 0.6$. Quasars with large redshift can only be observed if they are intrinsically powerful both optically and radio-wise: thus a spurious correlation between optical and radio luminosity is introduced if *all* quasars are plotted in this diagram. Moreover for quasars with large redshifts the effects of cosmological model and evolutionary hypothesis are very large. Fig. 5 shows luminosities as calculated in the Milne model, but the results are not very different for other models.

Fig. 5 shows clearly that there is no detailed correlation between optical and radio luminosities, so that the procedure described in Section 4 will be valid.

8. *An upper limit to the rate of luminosity evolution.* Before we proceed to test evolutions of the form (a)–(d), it is advisable to consider whether arbitrarily large

values of the parameters Q_L and z_L are acceptable. The effect of correcting the luminosities of all the sources is to reduce the value of $\hat{\mathcal{F}}(z)$ for any given value of z , by an amount which increases with z . In fact there is a value of z for which $\hat{\mathcal{F}}(z)$ reaches a maximum, decreasing for larger values of z . The consequence of this redshift falling within the range of redshift covered by our set of quasars can be seen from Fig. 6(a), (b), which show the optical and radio luminosity-

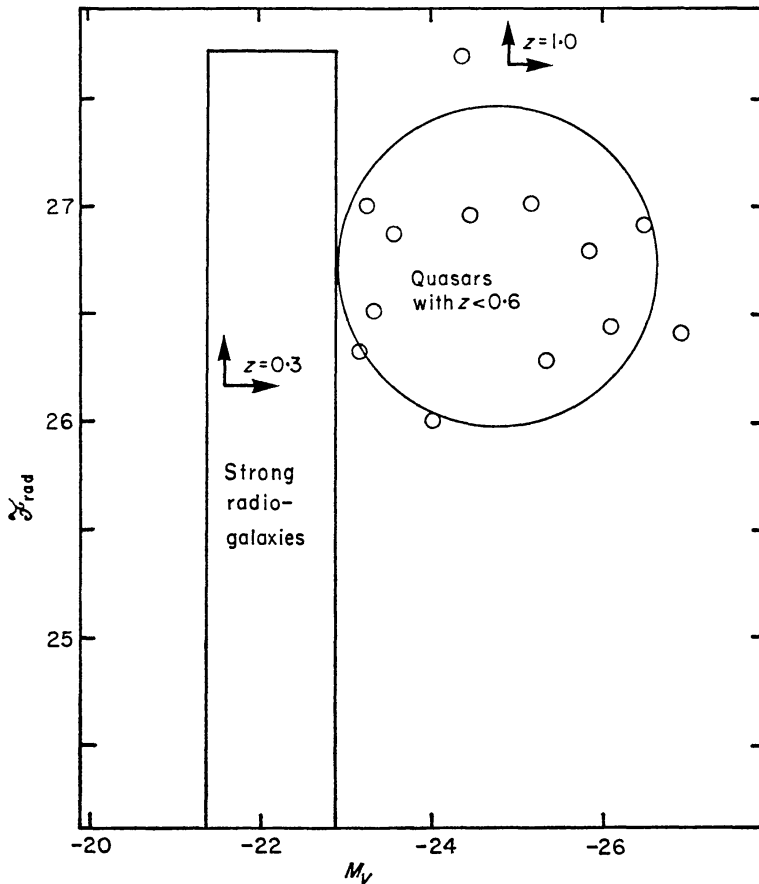


FIG. 5. Radio vs optical luminosity for quasars with redshift less than 0.6 (circles), calculated in the Milne model, showing absence of detailed correlation. The region of this diagram occupied by the strong radio-galaxies is indicated, as also are the cutoffs imposed by limiting optical and radio flux-levels of 19 m and 9 f.u. respectively on quasars with redshifts 0.3 and 1.0 respectively (a quasar with redshift 1.0, for example, must be above and to the right of the point of intersection of the arrows labelled ' $z = 1.0$ ').

volume diagrams for the Einstein-de Sitter model, corrected for luminosity evolution of form (a) with $Q_L = 3.07$. In this case $\hat{\mathcal{F}}(z)$ has a maximum at redshift 2.2, and if this form of evolution is correct then we should expect large numbers of quasars with redshifts greater than 2.2 and fluxes above the 3C limiting flux-level. Now although a sharp decline in the optical continuum emission beyond Lyman α (44) could explain the absence of such objects amongst those 3C sources identified with blue quasi-stellar objects, they should be visible as red stellar objects. Fig. 6(b) shows the effect of such a sharp cutoff (arbitrarily taken as $F(\nu) \propto \nu^{-5}$) on the distribution of visual luminosities. Clearly very many objects should be found in 3C with redshifts between 2.2 and 3.5 (note that the scale has been compressed beyond $U = 0.25$). Beyond $z = 3.5$, the radio-sources

would correspond to empty fields down to 19 magnitudes. Now although there are one or two tentative identifications of 3C sources with red stellar objects (45), and about 30 sources associated with empty fields (46), many of the latter are likely to be distant radio-galaxies. Thus the identifications of 3C do not permit large numbers of quasars beyond redshift 2.2, and evolutions so extreme as to

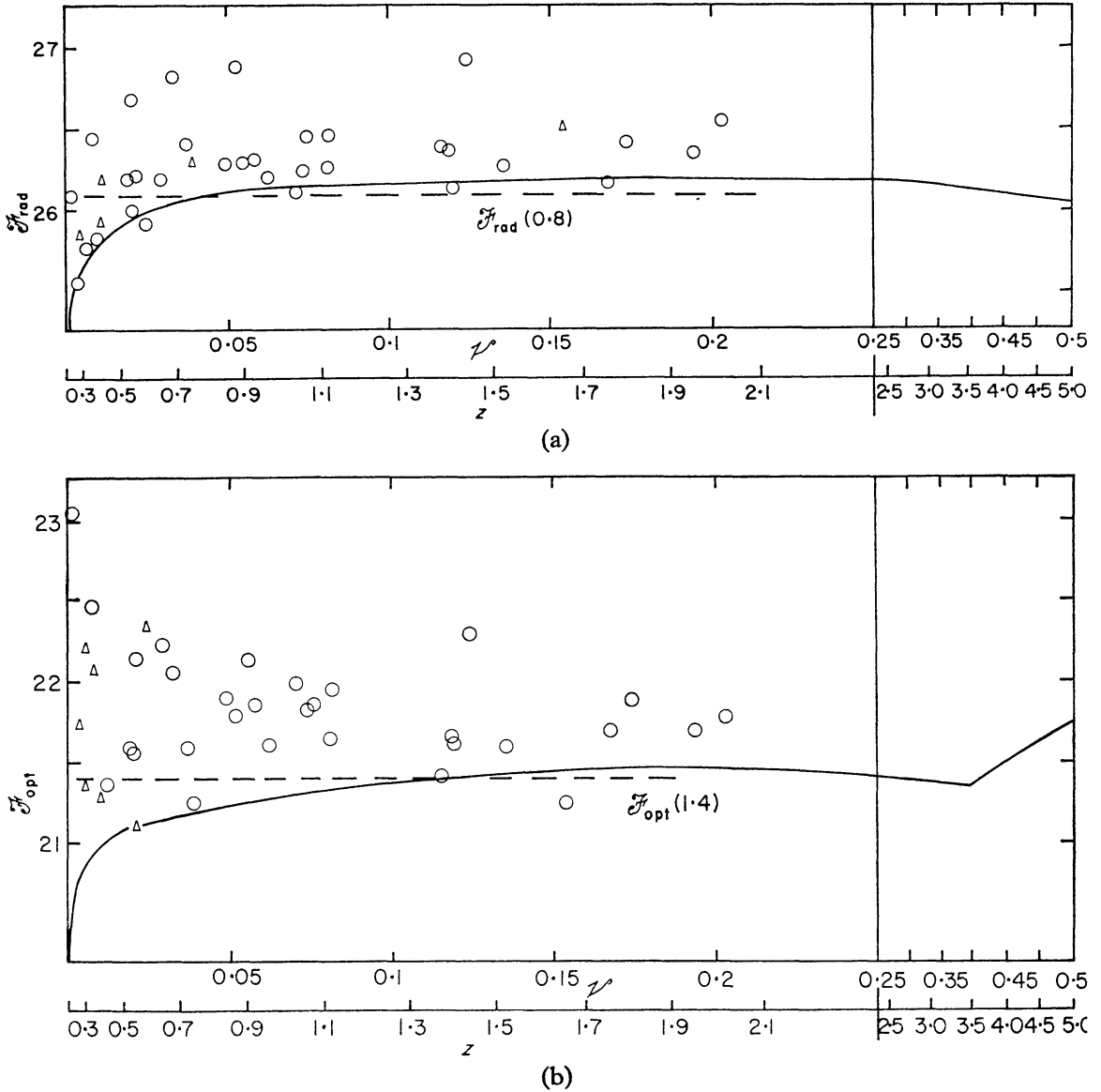


FIG. 6. As in Fig. 3, but the luminosities corrected for power-law luminosity evolution with $Q_L = 3.07$. The solid lines show cutoffs at nine flux-units and 19 magnitudes respectively, except that the effect of a sharp decline in the optical continuum beyond Lyman α is indicated in (b). Note that the volume scale is compressed beyond $z = 2.2$.

produce the situation illustrated in Fig. 6 can be ruled out. We are loath to introduce some *ad hoc* cutoff in the distribution of quasars beyond $z = 2.2$ until the less extreme models, where the radio cutoff provides a fairly natural explanation of the absence of 3C quasars beyond $z = 2.2$, have been eliminated.

Thus in any model we restrict our attention to values of Q_L and z_L for which the maximum in $\mathcal{N}(z)$ occurs at $z > 2.2$. This limitation is indicated by a dash-dotted line in Figs 4, 7-10.

Models which require Q_L or z_L less than but close to this limiting value are clearly unsatisfactory, by the same argument. For this reason the models in the top right-hand corners of Fig. 4(c), (d) are probably ruled out, even though they give consistency with the modified luminosity-volume test.

Finally, we may remark that it is a peculiarity of all models with luminosity evolution that the corrected luminosity of 3C273, the quasar with the smallest redshift in our set, is the largest of all: this peculiarity also applies to some cosmological models even without luminosity evolution (34).

9. *Correction for the incompleteness of the data for $V > 18$.* We can not hope to obtain accurate values for the evolutionary parameters if the selection effect postulated by Penston & Rowan-Robinson (3) is present. Without some such effect we have to admit that the quasars with large redshift are distributed anisotropically, so that analysis of the present kind is invalid. Since the quasars with $V > 18$ cover about half as much of the sky as those with $V \leq 18$, the simplest correction is to include each of the sources with $V > 18$ twice. Such a correction influences the radio luminosity-volume test only: the general effect is to increase the values of the evolutionary parameters slightly, though the results are not changed much qualitatively.

10. *Evolutionary parameters in the relativistic models.* Some of our results are summarized in Figs 4, 7-10. The models we have tested are as follows:

(i) a grid of models in the range: $-1 \leq q_0 \leq 3$, $0 \leq \sigma_0 \leq 3$; luminosity evolution (a) with $Q_L = 2.5, 3$ (Fig. 4(c), (d)),

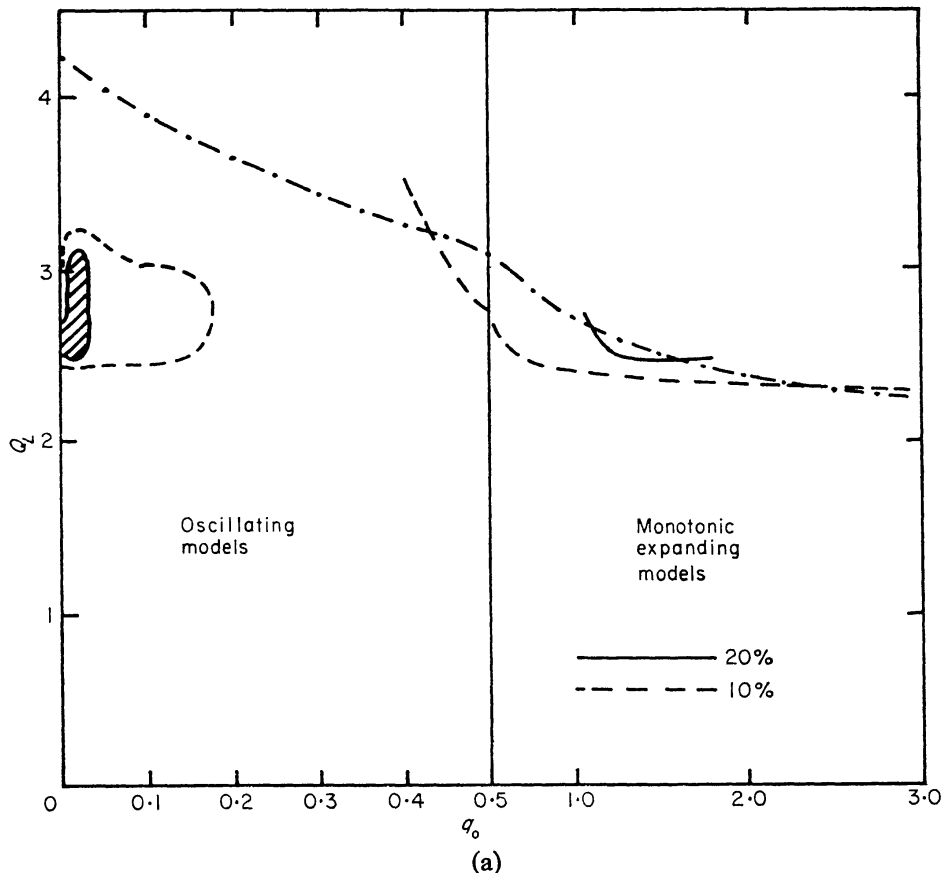
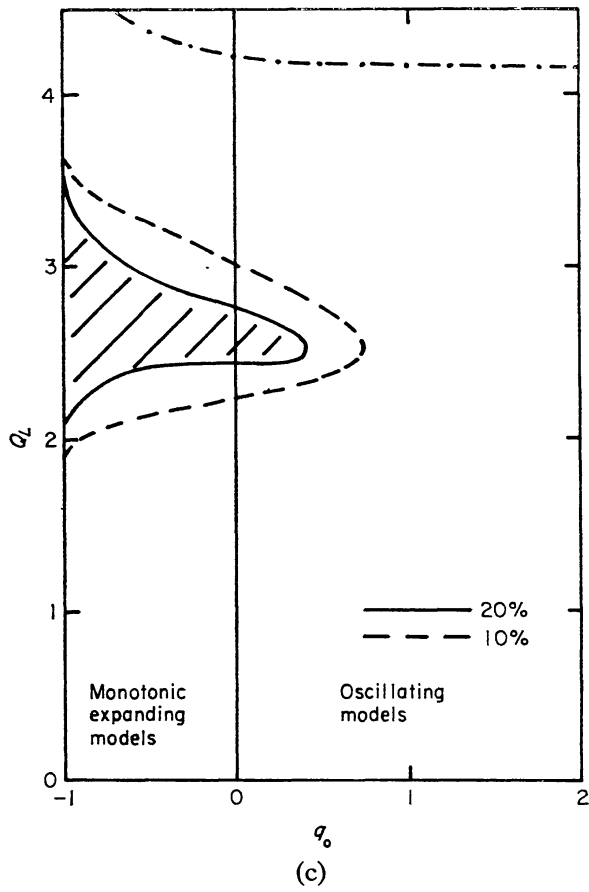
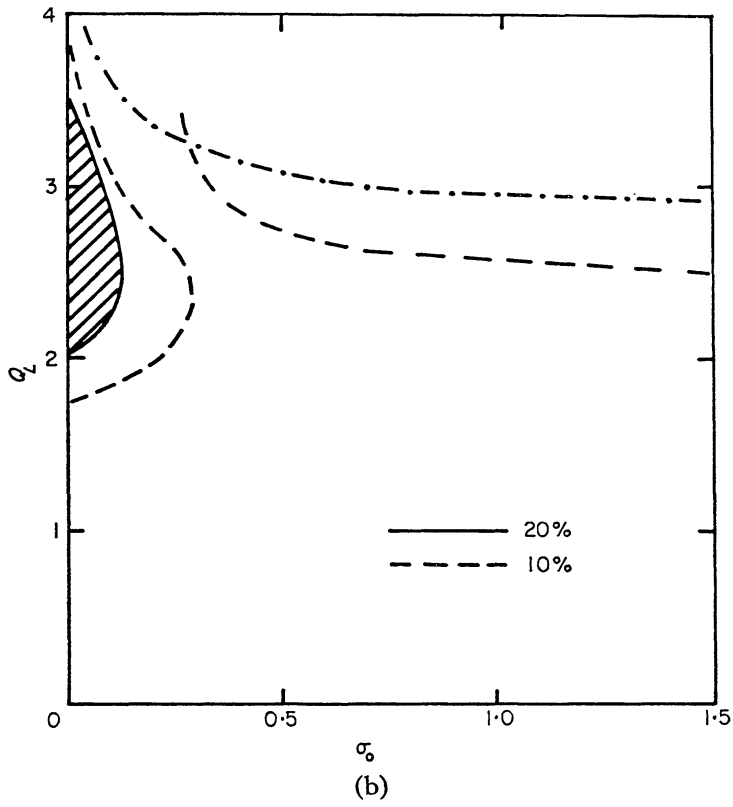


FIG. 7. Results of tests of models with power-law luminosity evolutions: (a) $\Lambda = 0$, $Q_L - q_0$; (b) $k = 0$, $Q_L - \sigma_0$; (c) $\sigma_0 = 0$, $Q_L - q_0$. Shaded regions correspond to models giving probabilities greater than 20 per cent of being correct.



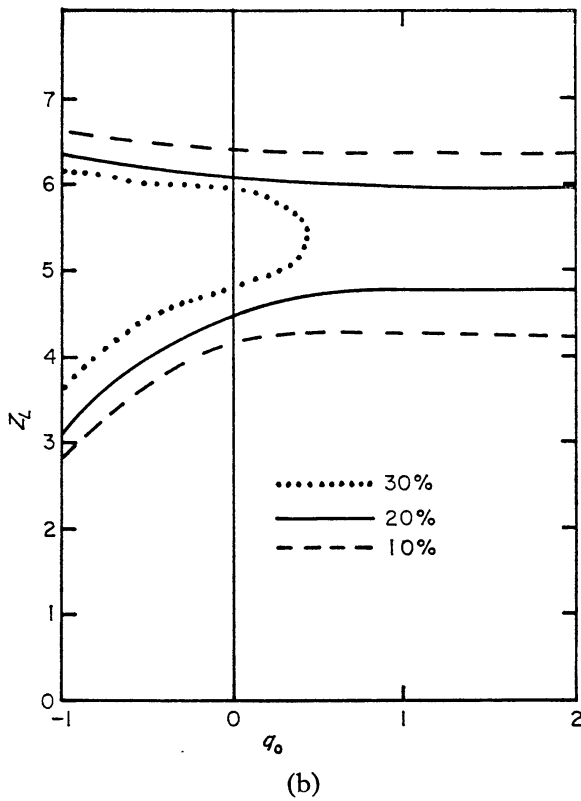
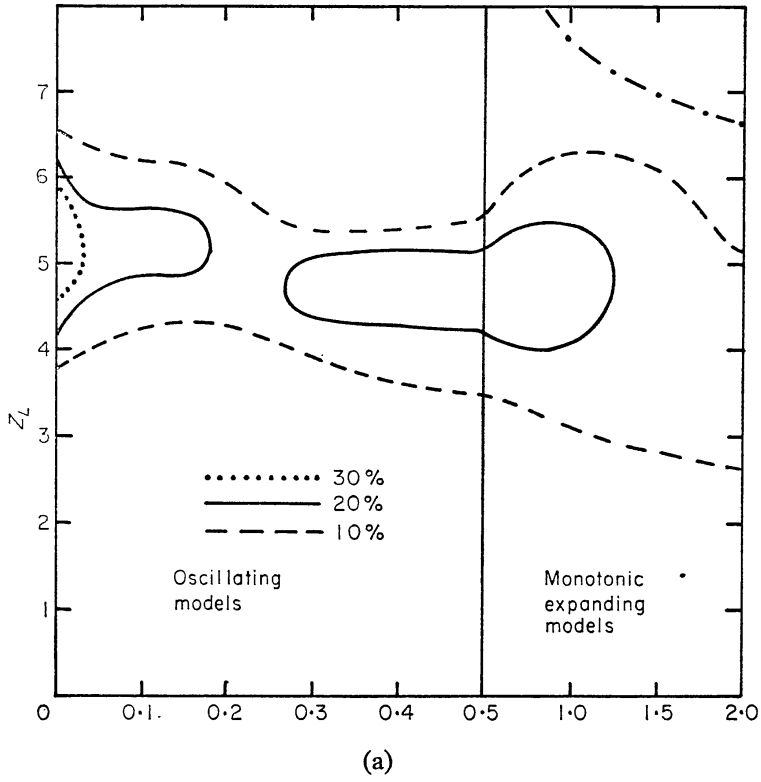


FIG. 8. Test of exponential luminosity evolution, $z_L - q_0$: (a) $\Lambda = 0$ (scale expanded for $q_0 < \frac{1}{2}$); (b) $\sigma_0 = 0$.

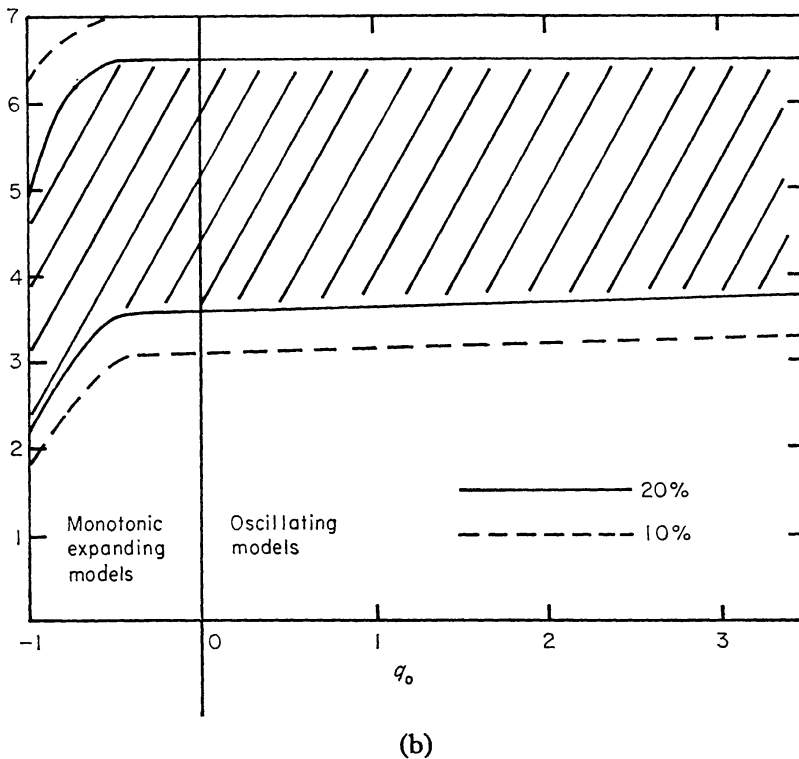
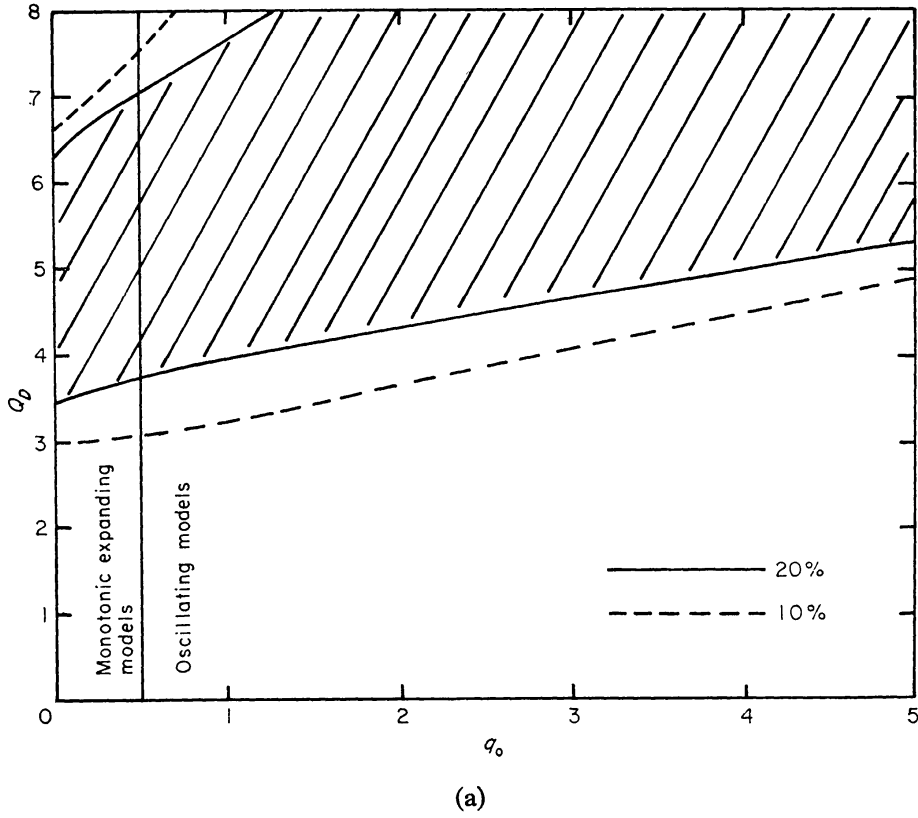


FIG. 9. Test of power-law density-evolutions, $Q_D - q_0$: (a) $\Lambda = 0$; (b) $\sigma_0 = 0$.

(ii) models with $\Lambda = 0$, $k = 0$, and $\sigma_0 = 0$ respectively; luminosity evolution (a) for a range of Q_L (Fig. 7(a), (b), (c)),

(iii) models with $\Lambda = 0$ and $\sigma_0 = 0$; luminosity evolution (b), and density evolutions (c) and (d) for ranges of the respective parameters z_L , Q_D , z_D (Figs 8(a), (b); 9(a), (b)),

(iv) de Sitter, Milne & Einstein-de Sitter models; combined evolutions of type (a) and (c) (Fig. 10(a), (b), (c)).

In each figure we show interpolated contours of 10 and 20 per cent probabilities that the present available data is consistent with the given model. Models giving probabilities below 10 per cent can probably be ruled out, even when the limitations

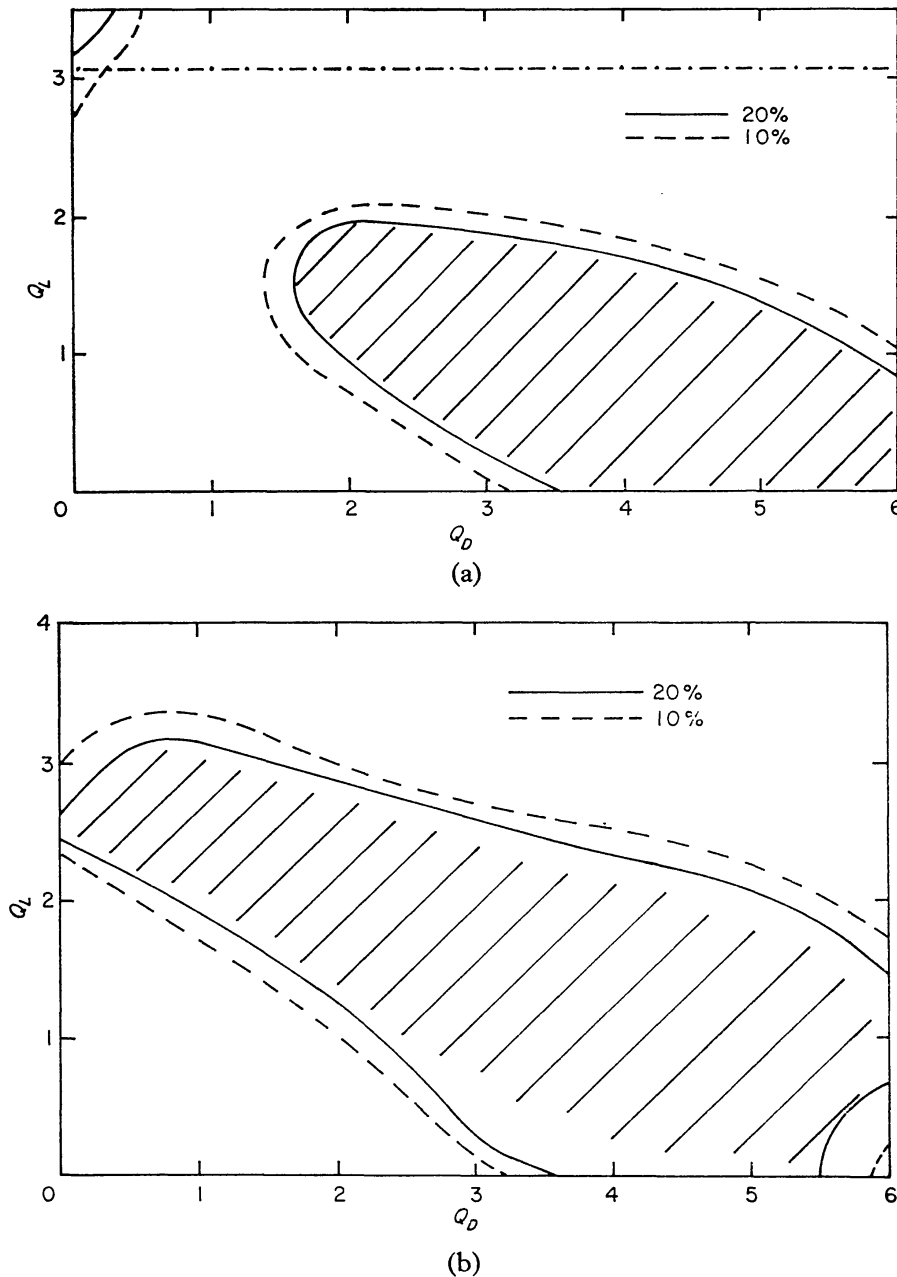
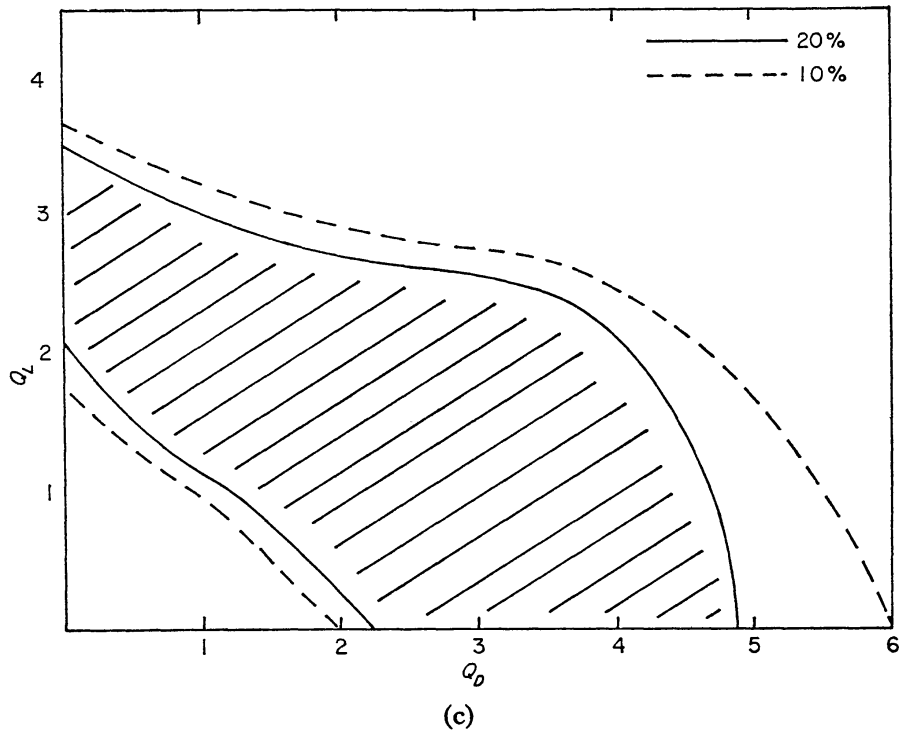


FIG. 10. Test of combined power-law luminosity and density evolutions, $Q_L - Q_D$: (a) Einstein-de Sitter, (b) Milne and (c) de Sitter models.



of the present work are borne in mind. We regard models giving probabilities higher than 20 per cent as acceptable, though many of these will almost certainly be ruled out when more complete data down to a lower flux-level is available. We discuss each of the four evolutionary hypotheses described in Section 6, in turn:

(a) Power-law luminosity evolution, which has been favoured by a number of authors, is the most vulnerable of the four hypotheses to this kind of analysis. There are few models in which this kind of evolution gives consistency with the data. Fig. 7(a) shows that of the models with zero cosmological constant, the only satisfactory models are those with q_0 close to zero. The best values for q_0 are in the range 0.005 to 0.03 , corresponding to a smoothed out density at the present epoch of 10^{-31} to 6.10^{-31} g cm³. The close agreement with values obtained from counting up the actual galaxies observed (30) should be regarded as coincidental until there are some strong grounds for believing that evolution of this kind is affecting the distribution of luminosities of quasars.

When a non-zero cosmological constant is included, the most satisfactory models are those with σ_0 close to zero (Figs 4(c), (d); 7(b)). Of the completely empty models by far the most satisfactory is the de Sitter model, and those with $q_0 > 1$ are ruled out. Thus exactly those models which might have been expected from consideration of the actual density of material observed to date, and from the problem of the long ages of the oldest stars, are preferred on this evolutionary hypothesis.

(b) Exponential luminosity evolution gives consistency with the data at the 10 per cent level for all the cosmological models tested to date (Fig. 8(a), (b)). In view of the advantage of this form of evolution already discussed, namely that no arbitrary truncation of the distribution is required, this result provides considerable incentive for further investigation of evolutions of this type. At the 20 per cent level models with $\Lambda = 0$, $q_0 > 1$, are ruled out, but all the empty

models are acceptable. For interest we show the 30 per cent contours also in Fig. 8(a), (b): these look very like the 20 per cent contours in Fig. 7(a), (b), suggesting that when more data is available, similar conclusions will be reached as for case (a). The best values for the parameter z_L are in the range 5 to 6: the significance of z_L is that between the epochs corresponding to $z = \infty$ and $z = z_L$ the typical luminosity of quasars has been reduced by a factor $1/e$. At the present epoch the typical luminosity is between 10^{-3} and $10^{-2.5}$ of the value at epoch $t = 0$.

(c) This analysis is extremely insensitive to power-law density evolution, in the sense that for all models quite a wide range of the parameter Q_D is consistent with the data (Fig. 9(a), (b)). Thus the earlier conclusion of the present author (24), that density evolution was at least as consistent with the data as luminosity evolution, can now be strengthened to the statement: *density evolution gives much better consistency with the data than luminosity evolution.*

We may note that of the models with zero cosmological constant, the empty models require the least severe evolution: and that of the empty models (including those with non-zero cosmological constant) the de Sitter requires by far the least severe evolution.

(d) Similarly insensitive results are obtained for exponential density evolution, with the best values of z_D being in the range 7–13. Here the significance of the parameter z_D is that between the epochs corresponding to $z = \infty$ and $z = z_D$ the fraction of material in the form of active quasars has decreased by a factor $1/e$. At the present epoch that fraction is only between 10^{-3} and 10^{-5} of the value at $t = 0$. If we consider quasars to be the birth-pangs of galaxies, then we may conclude that most of the galaxies had formed by the epoch corresponding to redshift 10 ± 3 .

The comparison of the Milne, de Sitter & Einstein–de Sitter models is very interesting (Fig. 10(a), (b), (c)). Density evolution alone is consistent with the data for all three models, as also are intermediate cases with combined luminosity and density evolution. Luminosity evolution alone is consistent with the de Sitter model for $2 \leq Q_L \leq 3.5$. For the Milne model a rather small range about $Q_L = 2.5$ is consistent: with more data a more detailed analysis may enable this possibility to be completely ruled out. For the Einstein–de Sitter model only values of Q_L which give rise to the difficulty discussed in Section 8 are consistent.

11. *Comparison with earlier work.* (i) Longair (18) has interpreted the Cambridge radio source-counts in terms of power-law luminosity and density evolutions of the most luminous sources, in the Einstein–de Sitter model. The best parameters he obtained ($Q_L = 3.3$, $Q_D = 5.7$) agree well with those obtained in this analysis of the available data for quasars, supporting his conjecture that the population causing the steep counts is the quasars. However, as we have remarked in the previous section, luminosity evolution with Q_L of order 3 or more in the Einstein–de Sitter model would require the existence of a large number of sources in 3C to be identified with quasi-stellar objects with redshifts greater than 2.2. This difficulty could only be overcome by supposing that there is a real truncation of the quasars at redshift 2.2: this value is significantly lower than the value required by Longair in his analysis ($z^* = 3$). This difficulty is less severe in the Milne and de Sitter models. Longair argues that the rapid change in slope of the $\log N$ – $\log S$ curve at low radio flux-levels is evidence of a real truncation at some epoch in the distribution of the sources. However, exponential evolution of the kind we have

TABLE II

$\log_{10} S$ ($\text{w m}^{-2} \text{ Hz}^{-1}$)	-24.0	-24.25	-24.5	-24.75	-25.0	-25.25	-25.5	-25.75	-26.0
$\frac{d(\log N)}{d(\log S)}$	-1.69	-1.76	-1.88	-2.10	-2.49	-2.98	-2.50	-1.08	-0.66

considered in Section 6 may also produce such an effect. Table II shows the number count slope as a function of flux-density for a set of sources uniformly distributed (coordinate number-density independent of epoch) in the Einstein-de Sitter model, when the sources at epoch corresponding to redshift z have luminosity of the form

$$10^{25.5} \left\{ \exp 6 \left(1 - \frac{1}{1+z} \right) \right\},$$

i.e. $z_L = 5$ in our notation of Section 6. Between 3 and 1 flux-units the number-count slope changes rapidly from -2.50 to -0.66 . This is even sharper than the observed change of slope, but it is clear that the dispersion in luminosity of the sources would smooth this out to some extent. More detailed analysis of the number-counts to low flux-level will be presented in a subsequent paper.

(ii) Davidson & Davies (21) have argued that the hypothesis of galactic collisions can be ruled out (without additional luminosity evolution) on the grounds of the source-counts, for models with $R(t) \propto t^{-n}$. While we do not necessarily wish to advocate this hypothesis, we note that this case, which corresponds to power-law density evolution with $Q_D = 3$, is not ruled out for the quasars in the de Sitter model. Of course the de Sitter model is not of the form considered by Davidson & Davies, but this demonstrates that the range of models considered by them does not necessarily include the full range of properties shown by the relativistic models.

(iii) Although the density-evolution hypothesis does not allow us to specify the cosmological model, we may compare the results obtained for the luminosity-evolution hypothesis (a) with those obtained using the brightest galaxies in clusters (29), (31)–(33). If the cosmological constant is set equal to zero, and allowance is made for the evolution of the stars in galaxies, both analyses agree in demanding a value for q_0 close to zero. When models with non-zero cosmological constant are considered our analysis gives the de Sitter as the most favourable model. For consistency of this model with the cluster data rather steeper optical luminosity-evolution would be required than has been considered to date (33).

12. Other cosmological models

(i) *The steady-state model.* Mathematically, the steady-state model is equivalent to the de Sitter model with negative power-law density-evolution, with $Q_D = -3$. The combined optical and radio luminosity-volume tests give a probability of only 0.01 per cent for this model.

(ii) *Brans–Dicke models with $k = 0$.* Brans & Dicke (47) have given the solution of the cosmological equations obtained from their scalar-tensor theory of gravitation for the case $k = 0$: the models are given by $R(t) \propto t^{(2+3\omega)/(4+3\omega)}$ where ω is a constant of the theory which can range from zero to infinity. As $\omega \rightarrow \infty$ these models tend to the Einstein-de Sitter model. We have tested these models for a range of ω : for $\omega \geq 4$ they give results identical to the Einstein-de Sitter model.

The value of ω inferred by Dicke from his interpretation of his measurements of the solar oblateness is about 6 (48). Thus there is little prospect of distinguishing between the rival theories of gravitation on the basis of cosmological tests.

13. *Conclusions.* If the redshifts of quasars are cosmological our tentative conclusions are that:

(i) No relativistic model is consistent with the data for quasars without some evolutionary factor that affects both radio and optical distributions.

(ii) The luminosity-evolution hypothesis is far more vulnerable to the luminosity-volume test than density-evolution.

(iii) Luminosity-evolution with a power-law dependence on the scale-factor requires $q_0 < 0.035$ if $\Lambda = 0$, with the best value being $0.005 \leq q_0 \leq 0.03$, or $10^{-31} \leq \rho_0 \leq 6 \cdot 10^{-31}$, in very good agreement with Oort's value (30) for the average smoothed-out density of matter in galaxies. If models with non-zero cosmological constant are also considered, the best models are those near to the de Sitter model in the σ_0 - q_0 plane, which give very long ages to the Universe.

(iv) Luminosity-evolution with an exponential dependence on the scale-factor gives better consistency with the data than power-law evolution, but the best models are the same as those given in (iii).

(v) Density-evolution gives consistency with all models, though the least severe evolution is required in the de Sitter model. With exponential evolution the epoch at which the number-density of quasars is $1/e$ times that at $t = 0$ is given by $z = 10 \pm 3$.

Some of these conclusions may be modified when all quasars in 3C have their redshifts measured, but it seems exceedingly unlikely that (i) and (ii) can be altered. These alone are sufficient to demonstrate the great power of the luminosity-volume test. While some of the features of this test have occurred independently to a number of authors (14), (35), (36), the two factors that enable significant conclusions to be reached are: allowance for selection effects imposed by the limiting flux-levels and the combination of the available information into a single probability.

14. *Future work.* Apart from the obviously urgent programme of the completion of redshift measurements of 3C quasars, important conclusions for cosmology may result from the following work:

(i) The completion of redshift measurements for 3C radio-galaxies, so that the radio luminosity-volume test may be applied. Here we do not have to add the proviso 'if the redshifts are cosmological', but the results may be less significant since we do not see galaxies out to nearly such large redshifts as quasars. At present the redshifts are 80 per cent complete for radio-galaxies with $m_v \leq 15$, but only 20 per cent complete for $15 < m_v < 20$.

(ii) Evolutions with exponential (and other?) dependence on the scale-factor should be investigated for consistency with radio number-counts to low flux-levels and the integrated extragalactic radio background.

(iii) It is a prediction arising from the present work that if the redshifts of quasars are cosmological, and the cosmology relativistic, then optical number-counts of quasars will be significantly steeper than 1.5. The results of optical searches for blue (or infrared (49)) quasi-stellar objects are awaited with interest.

(iv) Demonstration that the optical emission from quasars did not arise from a similar mechanism to the radio emission would throw considerable doubt on the luminosity-evolution hypothesis.

(v) Since there are more than ten times as many radio-sources per steradian brighter than the 4C (and Parkes) limiting flux-level than there are in 3C per steradian, it will be some time before the luminosity-volume test may be applied to these sources. Much more powerful conclusions may be expected, since the numbers will be sufficient to investigate the distribution of sources in the luminosity-volume plane in much more detail than our simple division of the observable region into two.

Clearly the observational programmes mentioned above are already being pursued. The present author hopes to present results bearing on (ii) in a subsequent paper: a rough preliminary version of the radio luminosity-volume test for radio-galaxies is also being performed, estimating the unknown redshifts from the optical magnitudes of the galaxies. Although crude, this should indicate whether significant results are to be hoped for, and thus whether the observational programme (i) is of high priority.

Acknowledgments. I would like to thank Mr M. V. Penston, Dr I. Roxburgh, and my supervisor, Professor W. H. McCrea, for stimulating discussions, and for helpful suggestions and criticisms. The computing was performed by the Computing Centre, University of Sussex, to whom thanks are due for much valuable assistance in the writing of the programs. I am indebted to the Science Research Council for a maintenance grant.

I am grateful to a referee for comments that enabled this paper to be improved.

*Astronomy Centre,
School of Mathematical and Physical Sciences,
University of Sussex.
1967 August.*

References

- (1) Greenstein, J. L. & Schmidt, M., 1964. *Astrophys. J.*, **140**, 1.
- (2) Strittmatter, P., Faulkner, J. & Walmesley, M., 1966. *Nature, Lond.*, **212**, 1441.
- (3) Penston, M. V. & Rowan-Robinson, M., 1967. *Nature, Lond.*, **213**, 375.
- (4) Burbidge, G. R. & Burbidge, E. M., 1967. *Astrophys. J.*, **148**, 107.
- (5) Arp, H., 1966. *Science*, **151**, 1214.
- (6) Arp, H., 1967. *Astrophys. J.*, **148**, 321.
- (7) Sandage, A. R., 1966. *Astrophys. J.*, **146**, 13.
- (8) Terrell, J., 1964. *Science*, **145**, 918.
- (9) Hoyle, F. & Burbidge, G. R., 1966. *Astrophys. J.*, **144**, 534.
- (10) Faulkner, J., Gunn, J. E. & Peterson, B. A., 1966. *Nature, Lond.*, **211**, 502.
- (11) Noedlinger, P. D., Jokipii, J. R. & Woltjer, L., 1966. *Astrophys. J.*, **146**, 523.
- (12) Hughes, R. G. & Longair, M. S., 1967. *Mon. Not. R. astr. Soc.*, **135**, 131.
- (13) Hoyle, F. & Burbidge, G. R., 1966. *Nature, Lond.*, **210**, 1346.
- (14) Kafka, P., 1967. *Nature, Lond.*, **213**, 346.
- (15) Ryle, M. & Clarke, R. W., 1961. *Mon. Not. R. astr. Soc.*, **122**, 349.
- (16) Davidson, W., 1962. *Mon. Not. R. astr. Soc.*, **123**, 425.
- (17) Gower, J. F. R., 1966. *Mon. Not. R. astr. Soc.*, **133**, 151.
- (18) Longair, M. S., 1966. *Mon. Not. R. astr. Soc.*, **133**, 421.
- (19) Davidson, W., 1962. *Mon. Not. R. astr. Soc.*, **124**, 79.
- (20) Davidson, W. & Davies, M., 1964. *Mon. Not. R. astr. Soc.*, **127**, 421.
- (21) Davidson, W., & Davies, M., 1966. *Mon. Not. R. astr. Soc.*, **134**, 405.

- (22) Longair, M. S., 1966. *Nature, Lond.*, **211**, 949.
 (23) Roeder, R. C. & Mitchell, G. F., 1966. *Nature, Lond.*, **212**, 165.
 (24) Rowan-Robinson, M., 1966. *Nature, Lond.*, **212**, 1556.
 (25) Robertson, H. P., 1933. *Rev. mod. Phys.*, **5**, 62.
 (26) McCrea, W. H., 1935. *Z. Astrophys.*, **15**, 69.
 (27) McVittie, G. C., 1956. *General Relativity & Cosmology*, Chapman & Hall, London.
 (28) Refsdal, S. & Stabell, R., 1966. *Mon. Not. R. astr. Soc.*, **132**, 379.
 (29) Solheim, J., 1966. *Mon. Not. R. astr. Soc.*, **133**, 321.
 (30) Oort, J. H., 1958. *Solvay Conference on La Structure et l'Evolution de l'Univers*, p. 163.
 (31) Humason, M. L., Mayall, N. U. & Sandage, A. R., 1956. *Astr. J.*, **61**, 97.
 (32) Baum, W. A., 1962. I.A.U. Symposium No. 15, *Problems of Extragalactic Research*, ed. by G. C. McVittie, p. 390.
 (33) Sandage, A. R., 1961. *Astrophys. J.*, **134**, 916.
 (34) McCrea, W. H., 1966. *Astrophys. J.*, **144**, 516.
 (35) McVittie, G. C. & Stabell, R., 1967. *Nature, Lond.*, **213**, 133.
 (36) Rees, M. J. & Sciama, D. W., 1966. *Nature, Lond.*, **211**, 1283.
 (37) Edge, D. O. *et al.*, 1959. *Mem. R. astr. Soc.*, **68**, 37.
 (38) Bennett, A. S., 1962. *Mem. R. astr. Soc.*, **68**, 163.
 (39) Rees, M. J. & Sciama, D. W., 1967. *Nature, Lond.*, **213**, 374.
 (40) Petrosian, V., Saltpeter, E. & Szekeres, P., 1967. *Astrophys. J.*, **147**, 1222.
 (41) Sandage, A. R., 1965. *Astrophys. J.*, **141**, 1560.
 (42) Burbidge, G. R., Burbidge, E. M., Hoyle, F. & Lynds, C. R., 1966. *Nature, Lond.*, **210**, 774.
 (43) Lynden-Bell, D., 1967. Herstonceux Conference on the Helium Problem.
 (44) Bahcall, J. N. & Sargent, L. W., 1967. *Astrophys. J.*, **148**, 165.
 (45) Wills, D. & Parker, E. A., 1966. *Mon. Not. R. astr. Soc.*, **131**, 503.
 (46) Veron, P., 1966. *Ann. Astrophys.*, **29**, 231.
 (47) Brans, C. & Dicke, R. H., 1961. *Phys. Rev.*, **124**, 925.
 (48) Dicke, R. H., 1967. *Phys. Rev. Lett.*, **18**, 313.
 (49) Braccresi, A., 1967, *Nuovo Cim. (B)*, **49**, 148.
 (50) Kellerman, K. I., 1964. *Astrophys. J.*, **140**, 969.
 (51) Pauliny-Toth, I. I. K., Wade, C. M. & Heesch, D. S., 1966. *Astrophys. J., Suppl. Ser.*, **13**, No. 116.
 (52) Kafka, P., 1967. Personal communication.

APPENDIX I

Radio and optical K-corrections

We write

$$f_{\text{rad}} = \log_{10} S_{178}$$

where S_{178} is the flux-density at 178 MHz in units of watts $\text{Hz}^{-1} \text{m}^{-2}$, taken from the 3C catalogue increased by 8 per cent (38), and take the radio K -correction to be

$$-0.4 K = (\alpha - 1) \log_{10} (1 + z)$$

where α is the spectral index in the range 178–750 MHz α is taken from Kellerman (50) in the case of those sources classified by him as having straight spectra: for the remainder of the sources α is calculated from the relation

$$\alpha = \frac{\log_{10} S_{178} - \log_{10} S_{750}}{\log_{10} 750 - \log_{10} 178}$$

where S_{750} is taken from Pauliny-Toth, Wade & Heesch (51). This procedure is exact for sources having spectra of the form $F(\nu) \propto \nu^{-\alpha}$, and is reasonably accurate even for sources with curved spectra, since the curvatures are not very great.

In order to convert the optical magnitudes to approximately the same absolute scale as the radio flux-densities, we write

$$f_{\text{opt}} = -22.4 - 0.4 V$$

where V is the apparent visual magnitude. We use the optical K -correction calculated by Sandage (52)

APPENDIX II

Calculation of \mathcal{F} and v

By definition

$$v(z) = \int_0^{r_0(z)} \frac{4\pi r^2 dr}{(1 + \frac{1}{4}kr^2)^3}$$

and

$$\begin{aligned} \mathcal{F} - f + 2.5 K &= 2 \log_{10} \left\{ \frac{r_0 R_0 Z}{1 + \frac{1}{4}kr_0^2} \right\} \text{ where } Z = 1 + z \\ &= 2 \log_{10} (R_0 v Z) \text{ where } v = \frac{r_0}{1 + \frac{1}{4}kr_0^2} \end{aligned}$$

From equations (2), (4) and (5) we find

$$\int_0^{r_0(z)} \frac{dr}{1 + \frac{1}{4}kr^2} = \frac{c}{R_0 H_0} \chi(z).$$

$k = +1$:

$$R_0 = c/H_0 \cdot (3\sigma_0 - 1 - q_0)^{1/2}$$

$$v = \sin \{ \chi \cdot (3\sigma_0 - 1 - q_0)^{1/2} \}$$

$$v(z) = 2\pi \{ \sin^{-1} v - v (1 - v^2)^{1/2} \}.$$

$k = 0$:

$$R_0 = c/H_0$$

$$v = \chi$$

$$v(z) = 4\pi v^3/3.$$

$k = -1$:

$$R_0 = c/H_0 (1 + q_0 - 3\sigma_0)^{1/2}$$

$$v = \sinh \{ \chi \cdot (1 + q_0 - 3\sigma_0)^{1/2} \}$$

$$v(z) = 2\pi \{ v(1 + v^2)^{1/2} = \sinh^{-1} v \}.$$

The cases where χ can be evaluated exactly are

$$\frac{\Lambda = 0:}{(q_0 \neq 0)}$$

$$\frac{R_0 H_0 v}{c} = \frac{q_0 z + (q_0 - 1) \cdot (\sqrt{1 + 2 q_0 z} - 1)}{q_0^2 (1 + z)}$$

$$\frac{\sigma_0 = 0:}{(q_0 \neq -1)}$$

$$\frac{R_0 H_0 v}{c} = \frac{\sqrt{(1 + q_0) Z^2 - q_0} - Z}{q_0}$$

The three asymptotic models are:

$$\sigma_0 = q_0 = 0 \text{ (Milne): } v = (Z^2 - 1)/2Z;$$

$$\sigma_0 = q_0 = \frac{1}{2} \text{ (Einstein-de Sitter): } v = 2(1 - Z^{-1/2});$$

$$\sigma_0 = 0, q_0 = -1 \text{ (de Sitter): } v = z.$$